UNCLASSIFIED

AD NUMBER

AD912492

NEW LIMITATION CHANGE

TO

Approved for public release, distribution
unlimited

FROM

Distribution authorized to U.S. Gov't.
agencies only; Test and Evaluation; JUL
1973. Other requests shall be referred to
Air Force Avionics Lab., AFSC,
Wright-Patterson AFB, OH 45433.

AUTHORITY

AFAL ltr, 15 Jan 1976

THIS PAGE IS UNCLASSIFIED

AFAL-TR-73-252

CHEMICAL VAPOR DEPOSITION OF MULTISPECTRAL WINDOWS

B. A. diBenedetto

J. Pappis

A. J. Capriulo

Raytheon Company
Waltham, Massachusetts

D D C

AUG 20 1973

C

TECHNICAL REPORT AFAL-TR-73-252

JULY 1973

Air Force Avionics Laboratory

Air Force Systems Command

Wright-Patterson Air Force Base, Ohio 45433

AD912492

NOTICE

CHEMICAL VAPOR DEPOSITION OF MULTISPECTRAL WINDOWS

B. A. diBenedetto

J. Pappis

A. J. Capriulo

D D C

AUG 20 1974

C

Distribution Statement

FOREWORD

This report was prepared by Raytheon Company, Research Division, Waltham, Mass., under Contract No. F33615-72-C-1501, Project No. 6102, entitled, "Chemical Vapor Deposition of Multispectral Windows." The work was administered under the direction of the Air Force Avionics Laboratory, Wright-Patterson Air Force Base, Ohio. Mr. C. T. Ennis (TEL) was task engineer.

At Raytheon, the investigation was carried on in the Advanced Materials Department of the Research Division. Dr. J. Pappis, Department Manager, and Mr. B. A. diBenedetto, principal investigator.

This is the Final Technical Report for Contract F33615-72-C-1501. It covers the period May 1972 to May 1973. The report was given the Raytheon internal number S-1580.

This report was submitted by the authors June 1973.

This technical report has been reviewed and is approved.

ROBERT E. DEAL
Laser & E-O Technology Branch
Electronic Technology Division

ABSTRACT

The significance of this research and development program to the Air Force is the demonstrated feasibility of fabricating zinc sulfo-selenide solid solutions for use as multispectral windows. Plates of 2 X 4 X 0.25 in. in size with good transmission properties over the entire spectrum were made and delivered. Furthermore, the strength and hardness of the solid solution is equivalent to zinc sulfide. Some improvement in homogeneity is needed, however, before an engineering material is available for systems use.

It was also shown that the hardness of pure zinc selenide could be increased by the use of oxygen or germanium. Finally, the amount of scatter in zinc sulfide was found to be dependent on deposition temperature, deposition rate, zinc usage rate, and the amount of gas phase reaction occurring during deposition.

TABLE OF CONTENTS

LIST OF ILLUSTRATIONS

LIST OF TABLES

SECTION I
INTRODUCTION

For the past ten years considerable effort has been devoted to developing materials for reconnaissance and weapon delivery systems that can operate over a wide electromagnetic spectral region. Currently these systems use several windows for the sensors to look through. The availability of a large-size multispectral window that would be capable of transmitting from the visible to the infrared ($\sim$0.5 to 13.5 μm) with the requisite physical characteristics to withstand environmental conditions would greatly simplify system design and space requirement problems.

One approach to fabricating a window material with these characteristics is through the use of the chemical vapor deposition (CVD) process. It has previously been shown that zinc sulfide and zinc selenide, two II-VI compounds, can be fabricated as plates in 1 X 2 ft. sizes. Optically, zinc selenide would make an excellent multispectral window. Because of its inherent softness and low strength, however, it would probably not survive environmentally. Zinc sulfide, on the other hand, will survive environmentally but because of scatter at visible wavelengths and intrinsic absorption beyond 10.5 μm is not satisfactory optically. One approach to fabricating a material that is both optically and structurally satisfactory is to alter the structural properties of zinc selenide by fabricating a solid solution where sulfur is partially substituted for the selenium. Calculations indicate that up to twenty (20) percent of sulfur can be substituted without detrimentally affecting transmission beyond 10.5 μm. A second approach to the problem is to substitute cadmium for zinc and form a zinc-cadmium sulfide solid solution. A third approach to the problem is to strengthen zinc selenide by precipitating a second phase (precipitation hardening). Finally, if zinc sulfide could be strengthened and its scatter at visible wavelengths improved it could be used in thinner cross sections and, in effect, transmit to a longer wavelength.

The program conducted at Raytheon Company explored all of the aforementioned material systems. A major part of the effort was devoted to the zinc sulfo-selenide solutions since these materials appear to offer the greatest potential. This part of the program was iterative in nature whereby changes were made in each run based on the evaluation of the previous run.

SECTION II
THE CHEMICAL VAPOR DEPOSITION PROCESS

The chemical vapor deposition (CVD) process offers many advantages over conventional techniques for preparing infrared transmitting materials. Perhaps the two most significant advantages are that the resulting material is very pure, thus eliminating IR absorptions due to impurities and that the deposits are usually very dense, and thus light scattering due to pores is minimized. Furthermore, the process is not inherently size limited and it has the potential of fabricating polycrystalline infrared windows in large sizes and various shapes.

The chemical vapor deposition process can be summarized as follows: Volatile compounds of the elements comprising the material to be deposited are reacted at a surface whose temperature allows the compound to decompose or react to form a solid, adherent coating. If the coating thickness is heavy enough a monolithic, free-standing plate is obtained. The volatile byproducts of the reaction are pumped away, flushed away in a stream of carrier gas, removed by reaction with a mass of suitable material in the system, or regenerated or used by reaction with a reservoir of a suitable raw material. Figure 1 schematically illustrates the apparatus used in this program.

Chemical vapor deposition processes can be used to form the most refractory substances at temperatures where their vapor pressure is negligible. The properties of the deposited materials can be significantly and controllably altered by the co-deposition of alloying atoms. Depending on the relative concentration of the reactants, either solid solutions or two-phase composites can be formed. Crystallite orientation and size distribution can be controlled by proper manipulation of the deposition parameters. Composites with alternating layers of two or more different materials can be prepared by cycling the composition of the vapors from which the materials are deposited.

Two general types of systems, static and dynamic, can be used for chemical vapor deposition. The static system is a closed system, in which the reactants and products are sealed in a chamber. Well-known examples are the quartz-iodine incandescent lamp and the hydro-thermal bomb for the deposition of synthetic quartz. In the dynamic system, on the other hand, fresh reactants are continuously metered into the deposition chamber, and the spent vapors are continuously removed, usually by pumping. The reactive gases are fed into the furnace through a gas-metering system. The substrate upon which the deposit occurs is maintained at an appropriate temperature by means of a heater that is inductively or resistively heated. Most vapor depositions are made at pressures on the order of one-hundredth of an atmosphere, although a much higher or lower pressure can be employed.

Our experiments have shown that the dynamic system yields good results in the deposition of zinc and cadmium sulfide and zinc selenide, and solid solutions of these materials, and is preferable because it offers certain advantages. Chief among these is the depletion of reactants and the accumulation of waste materials which are major problems in the static system, are minimal in the dynamic system which allows the addition and removal of materials during deposition. In order to obtain a deposit, the temperature of the substrate chamber and the vapor source are usually more critical and interdependent in the static system than in the dynamic system. The static system, in general, offers less flexibility in the deposition parameters than the dynamic system, since vapor transport is controlled by temperature gradients rather than pressure gradients and mass flow. In addition, the static system is often more susceptible to vapor phase nucleation and particle growth near the substrate; to reduce this effect the partial pressures of the reactive vapors must be low, resulting in low deposition rates. The reactive vapor concentrations are also limited by the equilibrium constants of regenerative reactions and by the fact that partial pressures of the regenerative vapor cannot (for safety reasons) usually greatly exceed one atmosphere. Finally, outgassing of deposition chamber and substrate are of greater importance in the static system than in the dynamic system.

Two general techniques can be employed in vapor deposition. These are: 1) Conventional chemical vapor deposition where the vapor source temperature is lower than the substrate temperature; 2) Transport chemical vapor deposition where the vapor source temperature is greater than the substrate temperature.

In conventional chemical vapor deposition, the thermodynamics and kinetics of the chemical reactions are such that formation of the solid product is favored at the higher temperatures, whereas the volatile reactants tend to be formed or are stable at the lower temperatures.

In chemical transport deposition, on the other hand, the thermodynamics and kinetics of the chemical reactions are such that formation of the solid product is favored at the lower temperatures, whereas the volatile reactants are formed at the higher temperatures. The deposition of II-VI compounds is best accomplished by use of the dynamic chemical vapor deposition technique. This method was used exclusively for the fabrication of the materials discussed in this report.

SECTION III
EXPERIMENTAL

1. INTRODUCTION

The experimental work performed on this program can most con-
veniently be broken down into four general groupings: zinc sulfo-selenide
solid solutions, zinc-cadmium sulfide solid solutions, improved zinc sulfide,
and impurity doping runs. In addition, diffusion experiments were carried
out in an attempt to diffuse dopants such as sulfur into zinc selenide, selenium
into zinc sulfide, as well as oxygen and other foreign dopants into "as depo-
sited" material. Finally, experimental work was carried out to increase
the surface hardness of zinc sulfide, zinc selenide and zinc sulfo-selenide
solid solutions by oxidizing the surface or sputtering zinc oxide onto the
surface.

The chemical vapor deposition apparatus used for this work is similar
to that described in previous studies on zinc sulfide under Contract No.
AF33615-71-C-1775. Figure 1 is a schematic of the reaction zone, input gas
train, and KOH scrubbing system used to react unspent gases. Modifications
were made to this apparatus to accommodate the various gases and the input
systems required to bring these gases to the reaction zones in the manner
desired. Details of the modifications are discussed when each system is
discussed.

2. ZINC SULFO-SELENIDE SOLID SOLUTIONS

Before the inception of this program zinc sulfide and zinc selenide
had been prepared by the CVD process at Raytheon. Further, it is a well
established fact that these two compounds will form a continuous solid solu-
tion. In these mixed crystals the long wavelength cutoff contains character-
istics of both the pure ZnS and ZnSe. The overall effect is to shift the multi-
phonon cutoff of ZnS to longer wavelengths as the percentage of selenium is
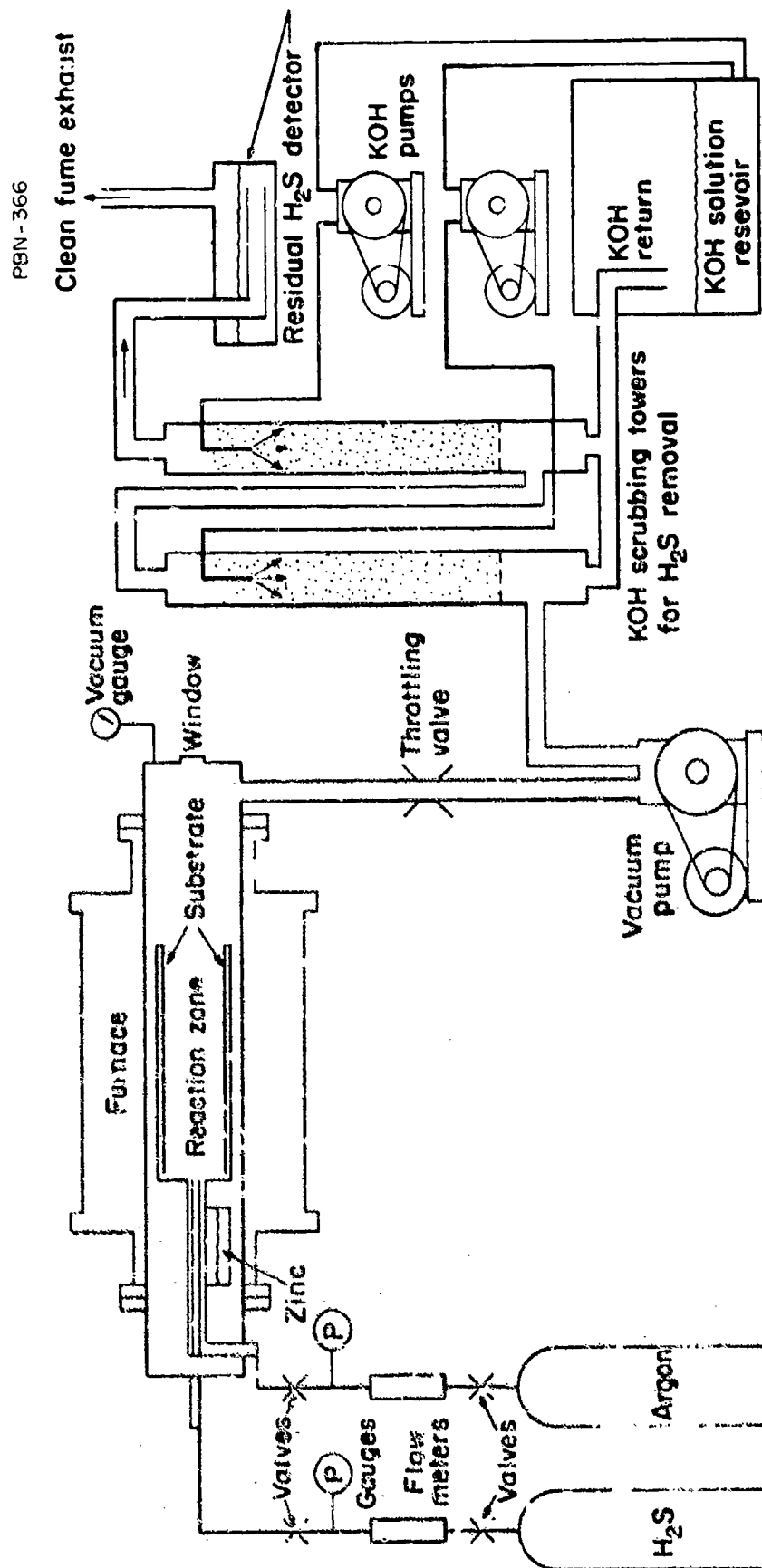
Fig. I Schematic of ZnS CVD system

PBN-366

7

is increased. The visible cutoff has a nonlinear dependence on composition, going from ~0.5 μm to ~0.4 μm as the percentage of sulfur is increased in ZnSe. In addition, all solid solution compositions should exhibit increased strength and hardness due to solid solution hardening phenomena.

Based on our previous work it was decided to deposit the solid solutions by reacting zinc vapor with hydrogen sulfide and selenide gases according to the reaction:

$$Zn(v) + xH_2S(g) + (1-x) H_2Se(g) \longrightarrow ZnS_xSe_{(1-x)}(s) + 2H_2(g)$$
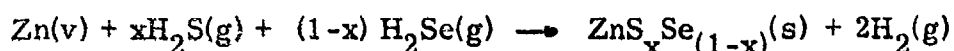
It is known that the dissociation kinetics of H_2S and H_2Se are dissimilar and that one could not expect the reaction rate of zinc and selenium (or a selenium compound) to be the same as the reaction rate of zinc and sulfur (or a sulfur compound). Therefore, fabrication of plates of 2 × 4 in. size with constant composition profiles would require some detailed examination of deposition composition as a function of H_2S and H_2Se gas input ratios, as well as the degree of premixing of these gases prior to reaction.

During the course of this program, nineteen (19) zinc sulfo-selenide depositions were made. The process parameters, i.e., mandrel temperature, furnace pressure, zinc retort temperature, gas flow rates etc. are given in Table I. The initial runs were used to determine process conditions that would yield a good imaging quality material and later runs were made for the purpose of preparing thicker plates as well as to improve the optical quality of material at higher sulfur concentration.

Initially, the reaction chamber system was designed with separate gas flow systems for the H_2S and H_2Se gas, while the zinc vapor was derived from a common source. Thus, it was possible to independently regulate the H_2S and H_2Se gas flows, and consequently the S:Se ratio in the reaction chamber. The first series of runs, ZSS-4, -5 and -6, were made in this way. In ZSS-4 the input H_2S and H_2Se gas ratio was 1:1, ZSS-5 was 3:1, and ZSS-6 was 9:1. These deposits were made at a deposition temperature of 650° C for 5 to 7

TABLE I

CVD Zn($S_{1-y}Se_y$) RUNS

Run No.	Mandrel Temp (°C)	Furnace Press. (torr)	Zn Retort Temp (°C)	H_2S Flow (lpm)	H_2Se Flow (lpm)	Deposition Time (hrs)	Zn Pick-up Rate (gm/hr)
ZSS-4	650	50	630	0.5	0.5	5.0	188
ZSS-5	650	50	640	0.75	0.25	7.0	160
ZSS-6	650	50	650	0.90	0.10	7.0	290
ZSS-7	650	50	650	0.75	0.25	7.0	306
ZSS-8	650	50	650	0.0	1.0	1.25	384
ZSS-9	750	60	590	0.02	1.0	7.0	---
ZSS-11	750	60	610	0.25	1.0	7.0	---
ZSS-12	750	60	610	0.5	0.5	10.0	---
ZSS-13	750	60	620	1.5	0.5	10.0	---
ZSS-14	750	60	620	0.6	0.4	10.0	---
ZSS-15	830	60	640	0.6	0.4	10.0	---
ZSS-16	750	60	610	0.5	0.5	10.0	180
ZSS-17	750	60	610	0.5	0.5	10.0	193
ZSS-18	750	60	600	0.5	0.5	10.0	113
ZSS-19	750	60	600	0.5	0.5	10.0	95.5
ZSS-20	750	60	590	0.9	0.3	10.0	57
ZSS-21	750	60	580	0.9	0.3	10.0	60
ZSS-22	750	60	590	0.5	0.5	24.0	80.5
ZSS-23	750	60	600	0.5	0.5	47.0	58.0

Table I (Cont'd)

Run No.	Mandrel Temp (°C)	Furnace Press. (torr)	Zn Retort Temp (°C)	H_2S Flow (lpm)	H_2Se Flow (lpm)	Deposition Time (hrs)	Zn Pick-up Rate (gm/hr)
ZS-116	610	40	590	1.0	- -	100.0	700.0
ZS-117	650	40	600	1.0	2.0†	24.0	120.0
ZS-118	650	40	600	1.0	0.1††	24.0	90.0
ZS-119	650	40	615	1.0	0.1††	18.0	90.0
ZSS-24	750	60	600	0.9	0.1	24.0	60.0
ZSS-25	650	60	600	0.9	0.1	24.0	30.0
ZSG-1	750	60	590	0.02*	1.0	7.0	- -
ZSG-2	750	60	590	0.1*	1.0	7.0	- -
ZSO-1	750	60	600	0.02**	1.0	7.0	- -
ZSO-2	750	60	600	0.5**	1.9	9.5	- -

† Substitute H_2 gas for H_2Se

†† Substitute O_2 gas for H_2Se

* Substitute germanium gas for H_2S gas

** Substitute oxygen gas for H_2S

10

hours duration and yielded material with poor imaging quality and poor compositional homogeneity as determined from property characterization studies carried out on each run.

The results of these early runs indicated that ZnSe was preferentially deposited. It was felt that if the H_2S and H_2Se were premixed a more homogeneous solid solution might be formed. Run ZSS-7 was made identical to ZSS-5 except that the H_2S and H_2Se gases were premixed external to the furnace. The resultant composition from this run was even higher in ZnSe indicating that reaction rates control the final composition. ZSS-7 also showed poor imaging quality and though the compositional gradient was improved with respect to ZSS-5 it still was measurably higher in selenium content in the first half of the reaction zone.

Run ZSS-8 was made to determine whether the deposition system used to deposit solid solution was the reason for the poor imaging quality of the solid solutions. The visible imaging quality of this run (ZnSe) was excellent, indicating that the problems being encountered were peculiar to the solid solution deposits, and were not due to geometric problems. X-ray data on runs ZSS-5, -6 and -7 showed that the solid solutions were being poorly formed and it was felt that this was at least partially because the deposition temperature was too low. Thus a deposition temperature of 750° C (temperature used to deposit ZnSe) was chosen for a new series of runs, ZSS-9, -11, -12, -13 and -14. Each of these runs had progressively more sulfur substituted for selenium in order to determine at what concentration of sulfur the imaging quality of the solid solution was degraded. The results of runs ZSS-9, -11, and -12 were quite encouraging. Excellent imaging quality material was deposited, hardness was improved, and the compositional gradient was reduced. Based on the results of these runs it appeared that the initial problems encountered were being overcome by the higher deposition temperature. ZSS-13 (a high sulfur concentration run), however, scattered significantly and therefore in run ZSS-14 the H_2S gas flow rate was again reduced. Analysis of this run indicated that the

11

scatter had not been significantly improved. However, when specimens perpendicular to the deposition surface were examined, "bands" were observed and it is known that these bands can cause poor imaging characteristics. The source of these bands is believed to be due to either nonuniform zinc vapor usage as a function of time or to gas phase reactions occurring for finite periods of time.

Since scattering at visible wavelengths had not been eliminated for high sulfur concentration material a run (ZSS-15) was made at 830° C in an attempt to fabricate scatter-free material. The results of this run indicated that deposition temperature per se does not decrease scattering since the imaging quality of this run was similar to ZSS-13 and -14.

In order to determine if the metal-vapor-to-gas (H_2S and H_2Se) ratio influenced scattering a series of runs was made at 750° C where the input ratio of H_2S:H_2Se was maintained at unity. In this series (ZSS-16 through -19) it was found that as the metal vapor pressure was decreased the imaging quality of the material continually improved. The composition of the material as determined by X-ray lattice parameters changed only slightly with the Zn-to-H_2S-H_2Se molar ratio but, in general, all the runs had 10 to 20 percent sulfur substituted for selenium. Runs ZSS-18 and -19 with the lowest zinc vapor flow rate exhibited the best imaging quality material.

In view of the fact that the imaging quality of the solid solution is a function of deposition temperature and zinc vapor partial pressure (in direct contrast with CVD ZnS results) another series of runs were initiated wherein the ratio of H_2S to H_2Se was again increased to potentially lower the cost of the material. Runs ZSS-20 and -21 were made at an input gas ratio of 3:1. These runs, as in the previous series, exhibited significantly improved imaging quality material with respect to run ZSS-13.

From analysis of the above depositions it appeared that a solid solution containing 10 percent sulfur, 90 percent selenium and deposited at 750° C

exhibited the best overall properties for the spectral ranges of interest
($\sim$0.5 to 12 μm). Thus it was decided to make two runs, ZSS-22 and -23,
to deposit material for property evaluation and for part of the deliverable
end-items due at the end of the program. Run ZSS-22 was of twenty-four
(24) hours duration and was terminated prior to its planned completion be-
cause of uncertainties in the zinc usage rate. This run yielded material of
approximately 1/8 in. thickness of excellent imaging quality. ZSS-23 was
set up and deposited for forty-seven (47) hours. The purpose of this run
was to deposit material of sufficient thickness to yield the desired plates.
It yielded excellent material which was used for the deliverable plates, as
well as for property evaluation measurements.

a. Compositional Analysis

The composition of the solid solutions was established by taking
representative samples from the top, middle, and bottom of each run and
determining their lattice parameters. A General Electric XRD-5 X-ray
diffractometer using CuKα radiation was employed for an initial scan. Then
representative high-angle diffraction peaks (usually the (620), (533), and (711)
peaks) were step-scanned at 200 sec per step using 2θ increments of 0.05°,
to obtain an accurate "d" spacing for lattice parameter calculations. This
parameter was then compared to a plot of the published values of solid solu-
tion composition as a function of lattice constant in order to identify the com-
position of the unknown sample. The lattice constants and composition of
each run are summarized in Table II.

In addition to the composition, the X-ray data yielded information
about the homogeneity of the solid solutions that were deposited. Figure 2
shows a series of (620) diffraction peaks for a set of samples that have pro-
gressively poorer homogeneity. Figure 2a is a diffraction peak for pure
ZnSe and the increasing broadness of the diffraction peaks in Figs. 2b and c
indicate that the composition range is becoming progressively wider. Finally,
in Fig. 2d there are two broadly overlapping peaks, indicating that this deposit
contained two discrete composition distributions. It is theorized that one

TABLE II

LATTICE PARAMETERS AND COMPOSITION OF ZSS RUNS

| Run No.	Mixing Chamber Param., Å	Mixing Chamber % ZnS	Bottom Mandrel Param., Å	Bottom Mandrel % ZnS	Middle Mandrel Param., Å	Middle Mandrel % ZnS	Top Mandrel Param., Å	Top Mandrel % ZnS	Exhaust Chamber Param., Å	Exhaust Chamber % ZnS
ZSS-4	---	---	5.643	91.0	5.646	92.0	5.485	31.5	---	---
ZSS-5	---	---	5.42-5.51	85-59	5.448	82.0	5.454	80.0	---	---
ZSS-6	---	---	5.43	89.0	5.45	81.0	5.46	78.0	---	---
ZSS-7	---	---	5.65	7.0	5.65	7.0	5.62	28.0	5.53	52.0
ZSS-8	---	---	---	---	5.669	< 1.0	---	---	---	---
ZSS-9	---	---	---	---	5.667	< 1.0	---	---	---	---
ZSS-11	5.664	1.5	---	---	5.666	0.5	---	---	---	---
ZSS-12	5.661	21.0	---	---	5.639	11.0	---	---	---	---
ZSS-13	---	---	---	---	5.598	26.0	---	---	---	---
ZSS-14	---	---	5.589	89.5	5.631	14.0	5.623	17.0	---	---
ZSS-15	---	---	5.57-5.98	37-26	5.575	35.0	5.566	38.0	---	---
ZSS-16	---	---	---	---	5.634	13.0	5.639	11.0	---	---
ZSS-17	---	---	5.595	27.0	5.61	22.0	5.612	21.0	---	---
ZSS-18	---	---	---	---	5.646	8.0	---	---	---	---
ZSS-19	---	---	5.645	8.5	5.648	7.5	5.645	8.5	---	---
ZSS-20	5.634	13.0	5.616	19.5	5.616	19.5	5.610	22.0	---	---
ZSS-21	---	---	5.608	22.5	5.625	16.0	5.614	20.0	---	---
ZSS-22	---	---	5.641	10.0	5.648	7.5	5.648	7.5	---	---
ZSS-23	---	---	5.650	7.0	5.652	6.0	5.651	6.5	---	---
ZSS-24	---	---	---	---	---	---	5.458	78.0	---	---
ZSS-25	---	---	---	---	---	---	---	---	5.429	89.0
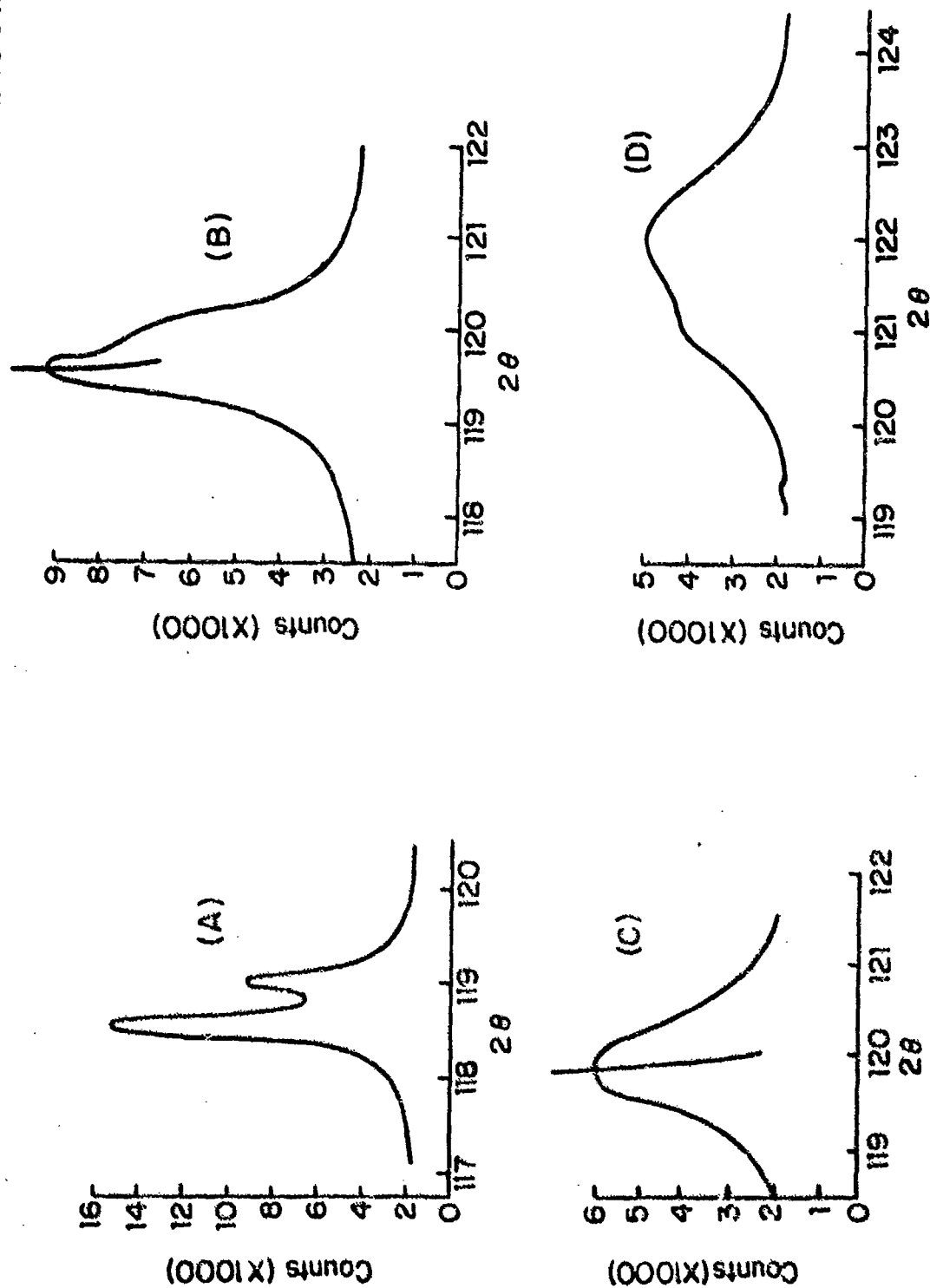
Fig. 2   (620) High-Angle X-Ray Diffraction Peak of Progressively
         Less Homogeneous Solid Solutions

composition is the result of a vapor phase reaction, while the other composition was formed at or near the mandrel surface.

In all cases the composition of the solid solution is high in selenium as compared to the composition of the reactant gases immediately adjacent to that area of the mandrel. In the early runs, ZSS-4 through -7, there was also a large spread in composition from one end of the mandrel to the other, as shown in Table II. In subsequent runs, however, this compositional gradient was minimized (to $\sim \pm 1\%$). This was especially true in the good imaging quality runs ZSS-9, -11, -12, -18, -19, -22, and -23. It appears, in fact, that poor compositional homogeneity and/or compositional gradients are a characteristic of poor imaging quality runs, lending credence to our contention that vapor phase reactions are one of the causes of scattering centers in solid solutions.

b. Transmission

The in-line transmission from 2.5 to 40 μm was measured on polished samples taken from the top, middle, and bottom of each deposit. A Perkin-Elmer 457 Grating Infrared Spectrometer was used for this purpose. The aperture size is approximately 0.2 in^2 and sample thickness varied from 0.007 to 0.250 in. depending on the thickness of the deposit.

The initial series of runs, ZSS-4 through -7, produced the spectrum of solid solutions desired. The in-line transmission of typical samples from this series of runs, shown in Fig. 3a and b, demonstrate the change in the position of the multiphonon absorption band edge. Because of the short deposition times used some of the samples after polishing were thin ($\sim$0.009 in. thick) and considerable detail of the long wavelength bands is seen. The two transmission spectra show the two types of spectra that emerge when sulfur is added as a dopant to zinc selenide and vice versa.

Figure 4 summarizes the degree to which the multiphono absorption edge can be altered in this system. Samples which represented the total

16

PBN-73-701

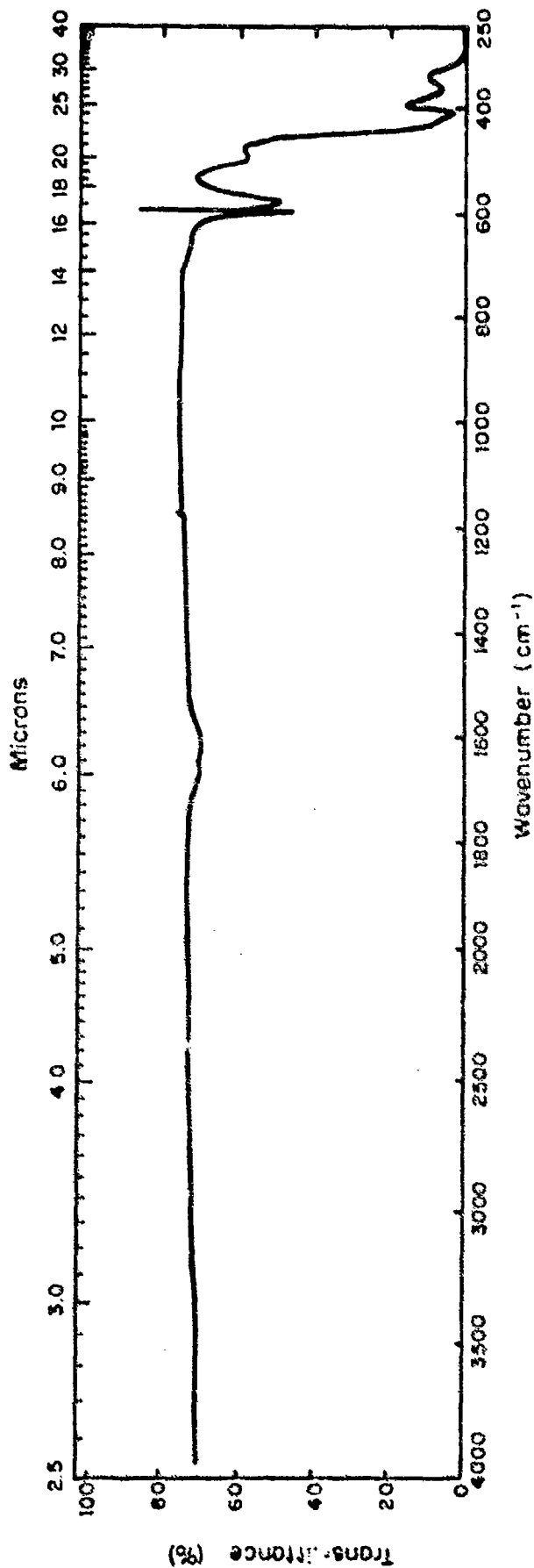Fig. 3a   IR Transmission for $Zn(S_{0.1}Se_{0.9})$ Run ZSS-4, Thickness 0.0095 in.
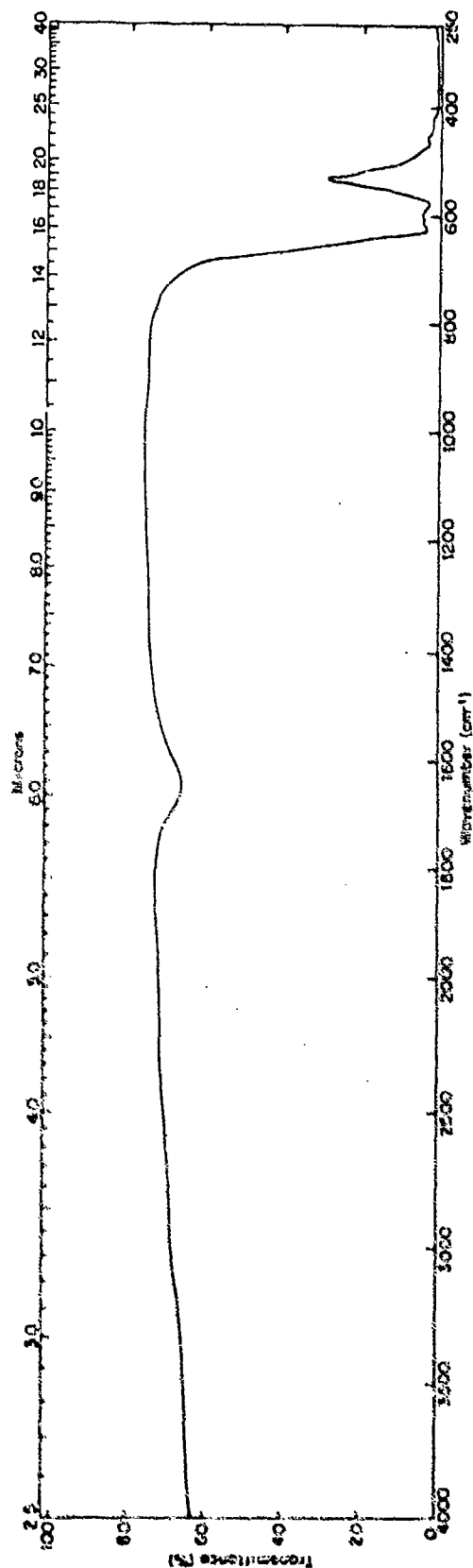
Fig. 3b   IR Transmission for $Zn(Se_{0.19}S_{0.81})$ Run ZSS-6, Thickness 0.030 in.
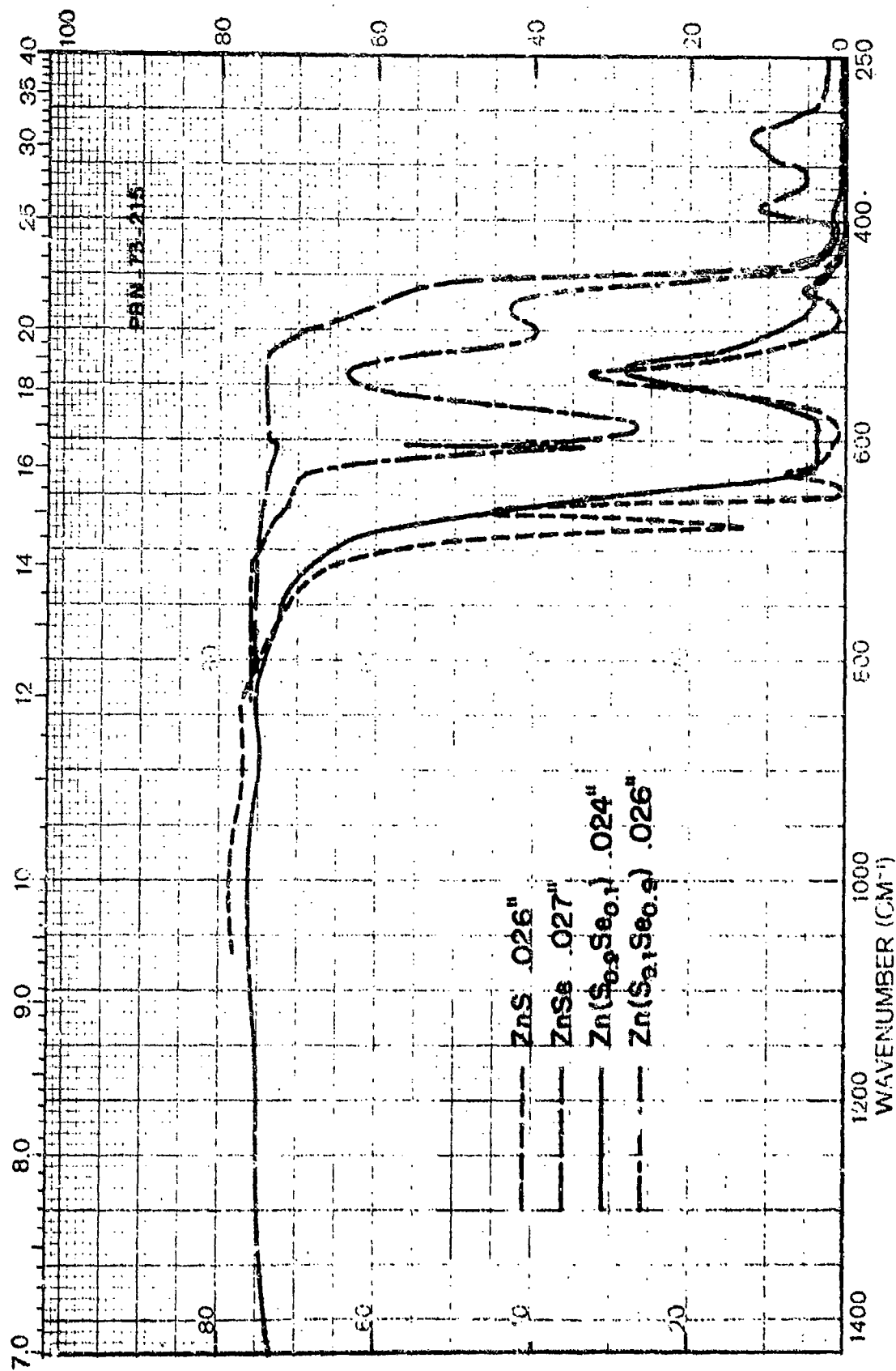
17

Fig. 4   IR Transmittance as a Function of Composition in the System $Zn(S_x Se_{1-x})$

composition range from ZnS to ZnSe were prepared to approximately the same thickness (0. 025 in.). When small amounts of sulfur are substituted for selenium in zinc selenide, an apparent impurity absorption band begins to appear at approximately 17 μm. Conversely, a small amount of selenium substituted for sulfur in zinc sulfide appears to annihilate the small intrinsic absorption peak in zinc sulfide at approximately 15 μm.

One of the limitations of CVD ZnS is its intrinsic absorptions beyond 10. 5 μm. In thick samples (> 1/4 in.) the absorption is appreciable and limits the usefulness of the material in the 8-12 μm range. Figure 5 illustrates the changes in the multiphonon region as a function of selenium content in zinc sulfide for samples of approximately 0. 2 in. thickness. The surface reflection losses for all these materials were cancelled so that these transmission curves allow a direct comparison of absorption vs composition. It is also possible to see that the 11 μm absorption band in zinc sulfide shifts progressively to longer wavelengths as selenium is substituted for sulfur. Considering all properties including scatter in the visible, a solid solution containing 10 percent sulfur $(ZnS_{0.1}Se_{0.9})$ is the best candidate for a multispectral window at this time. Figure 6 shows the additional transmission (shaded area) one can expect for 0. 250 in. thick windows of this composition. On the other hand, if only the 8-12 μm range were of interest, the available transmission, hardness, and strength data would suggest a 20 mole percent replacement of selenium with sulfur as the overall superior material.

Figures 7 and 8 show in-line transmission spectra for ZnSe, ZnS, and a $ZnS_{0.1}Se_{0.9}$ solid solution from the visible band edge through the multiphonon absorption band. As noted from these traces, the ZnSe transmission rises rather sharply and remains relatively constant to approximately 14 μm. The transmission curves for ZnS and $ZnS_{0.1}Se_{0.9}$, on the other hand, do not rise as rapidly at the low wavelengths indicating that absorption and scattering are occurring in this range. However, visible imaging through the solid solutions is significantly better than imaging through ZnS. Beyond 2. 0 μm both materials are free of extraneous absorptions and scatter in the spectral range of interest.

19
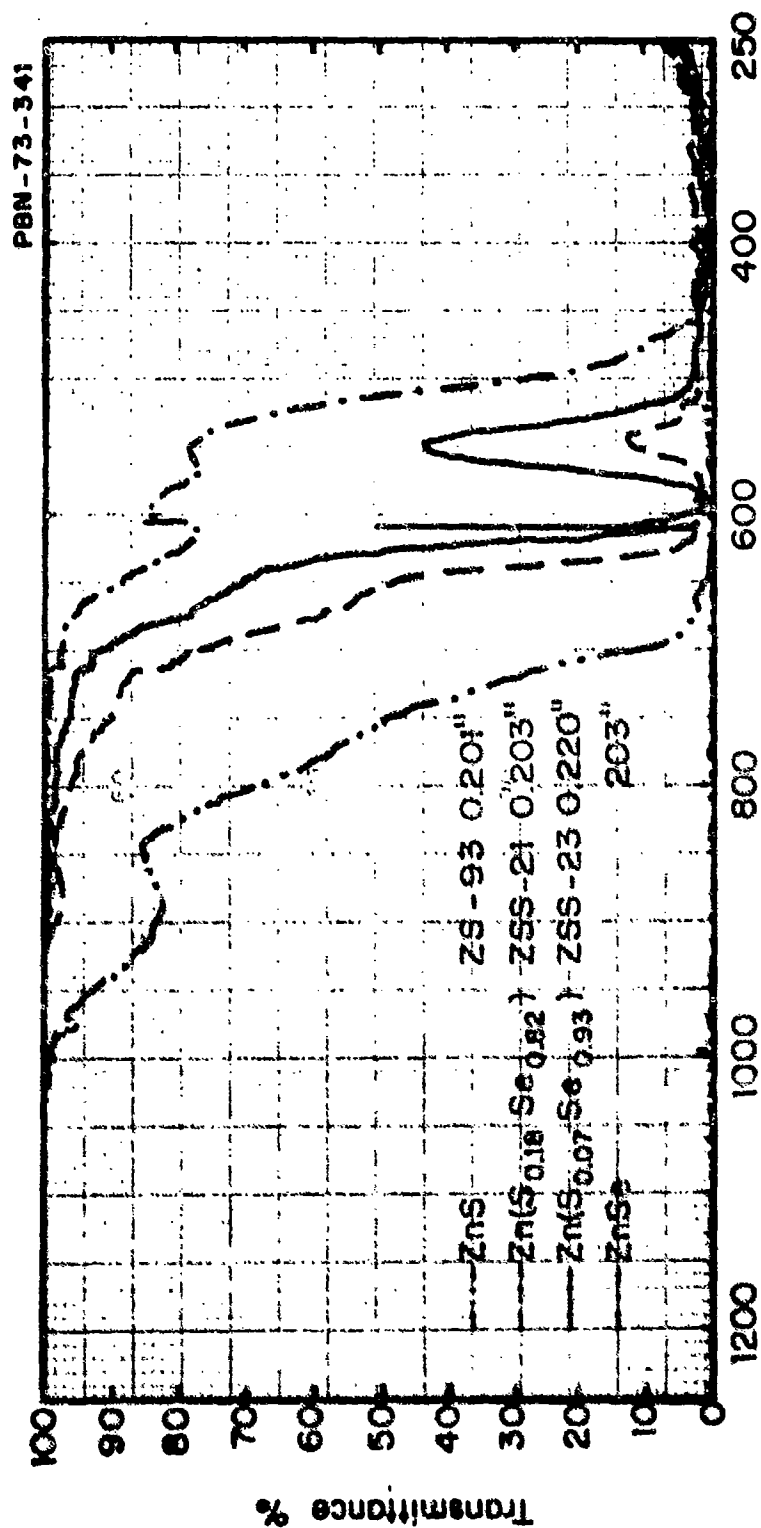
Fig. 5   In-Line Transmission of ZnS, ZnSe Sulfo-Selenide
          Solid Solutions

20
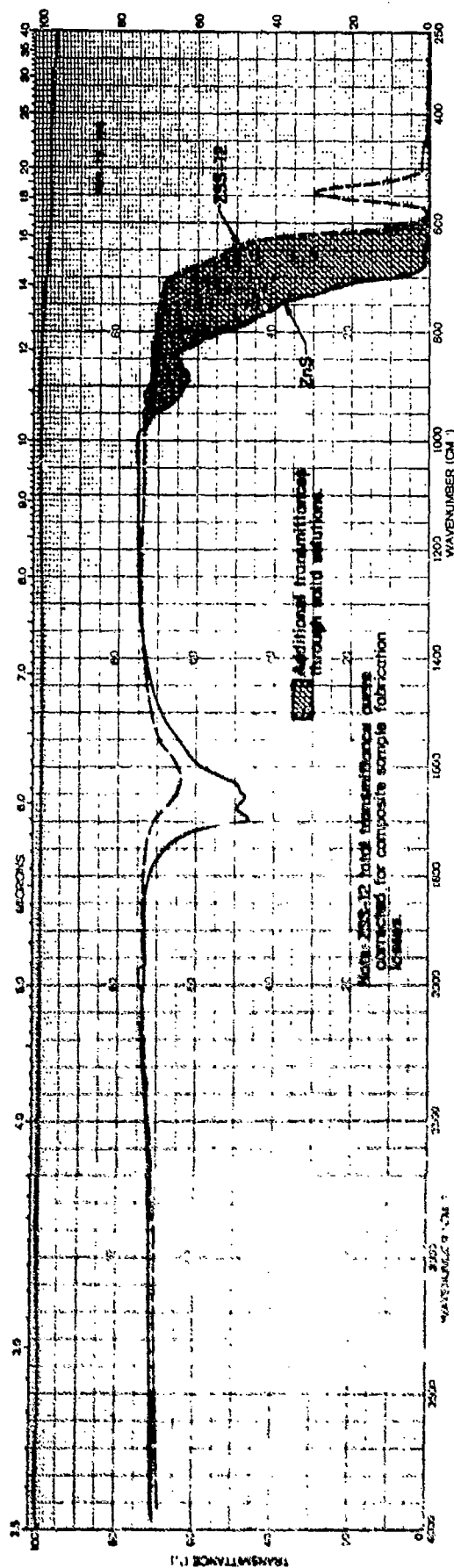
Fig. 6   Transmittance of ZnS and ZSS-12 Demonstrating Improved 10.0 → 14.0 μm Absorption (both samples 0.250 in. thick)
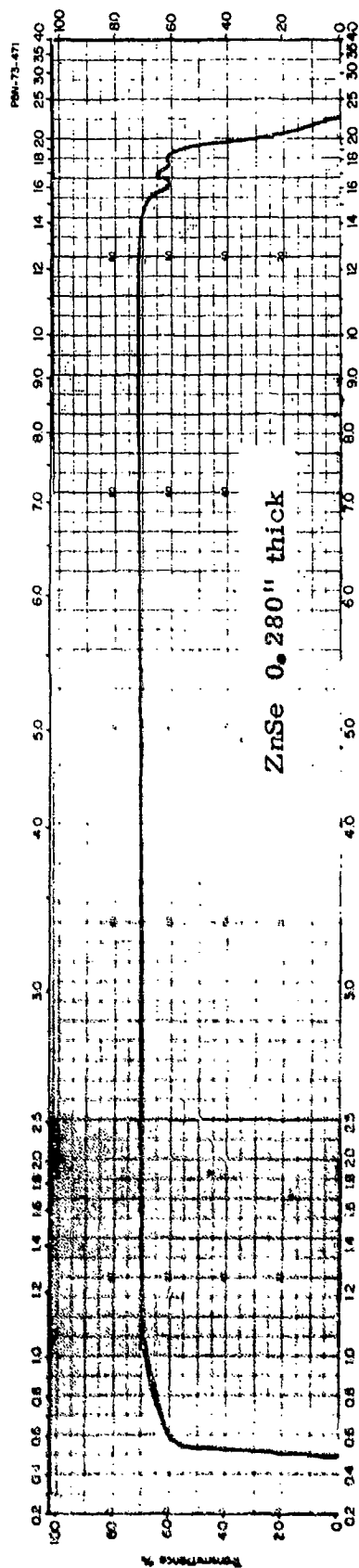
Fig. 7a   Typical In-Line Transmission Curve (0.5 to 22 μm)
           for CVD ZnSe
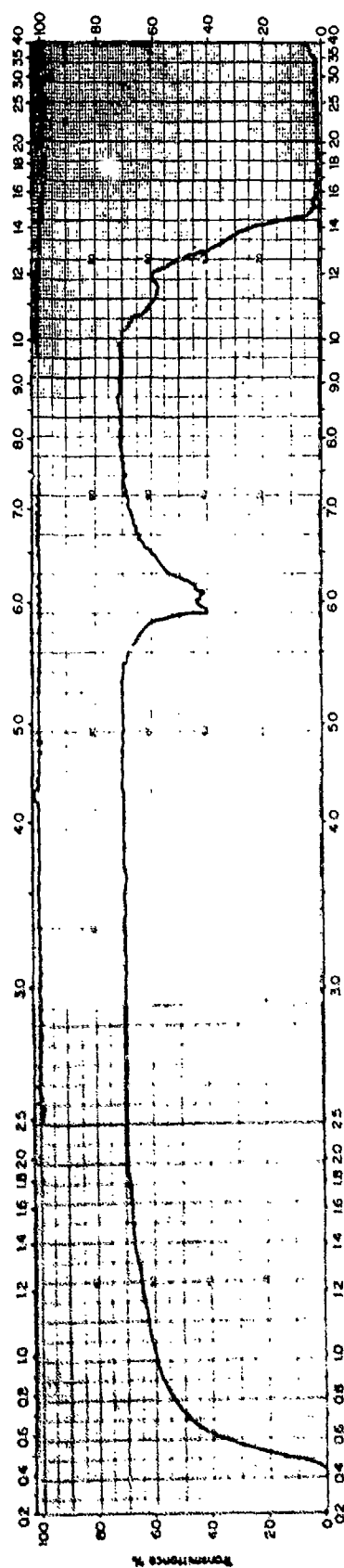
Fig. 7b   Typical In-Line Transmission Curve (0.5 to 14 μm) for CVD
           ZnS taken from a Large Plate Run, t = 0.202 in.

22
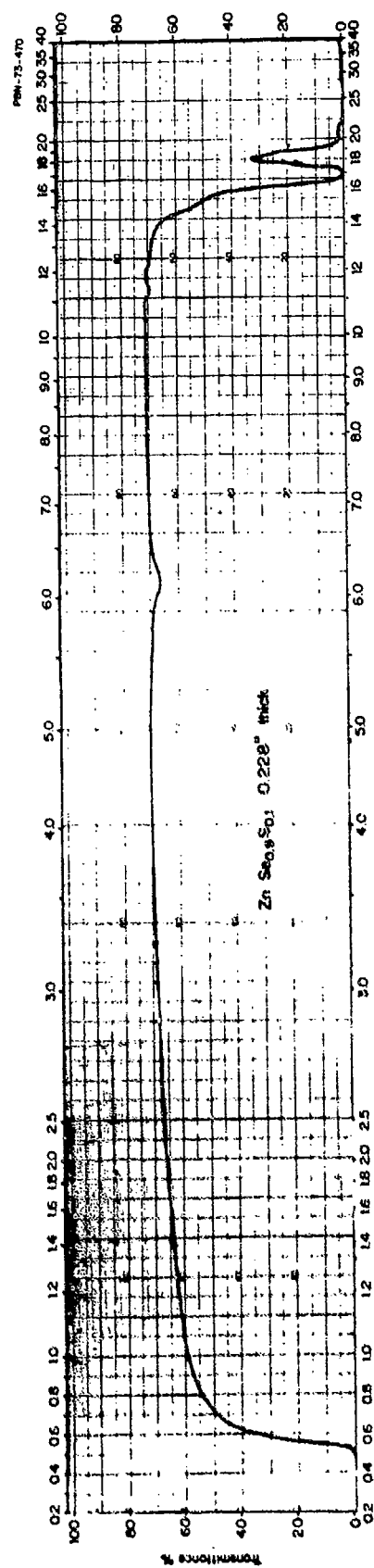
Fig. 8   Typical In-Line Transmission Curve (0.5 to 22 μm)
for CVD Zinc-Sulfo-Selenide Solid Solution

23

In examining the imaging characteristics of the solid solution deposits perpendicular to the deposition plane, bands of a differing index of refraction are seen. These bands are potentially quite bothersome. The degree to which this can be a problem is shown in the following analysis. The refractive index of zinc sulfide is 10 percent lower than that of the selenide (2.20 vs 2.40) in the 8-13 μm range used in long wavelengths passive i.r. systems. The refractive index of a specific solid solution can be estimated by simple linear interpolation between these two limits. Thus a 10 percent sulfide substitution would result in a refractive index near 2.38.

Refractive index variations in the end members ZnS and ZnSe can be produced only by impurities or by nonuniform porosity. Both of these are unlikely, and in fact the measurements already made on ZnSe show an rms refractive index variation, $\overline{\Delta \eta}_{rms}$, of less than 1.0×10^{-5}. At this level, we are dealing with very high optical quality material, even for use in the visible wavelength range. For use in present operational infrared systems, a value of 10^{-4} is required for adequate i.r. image definition. CVD zulfide and selenide separately meet this requirement with ease.

In sulfo-selenide solid solutions, compositional variations can produce a refractive index variation more important than the relatively trivial density changes. A 1 percent variation in an absolute sulfide concentration will produce a change of 2×10^{-3} in refractive index. Thus an rms transverse compositional change of 5×10^{-4} or less is required to keep the rms refractive index to the desired level of 10^{-4}. This is a very tight restriction, and is unlikely to be met at all times during a deposition. Fortunately, the restriction in refractive index change can be relaxed substantially if that variation occurs in a direction normal to the plane of an optical surface, that is, along the appropriate ray direction. Fortunately, this is the situation in stratified CVD materials. Furthermore, if the lateral variations, when they do occur, are in high spatial frequencies, that is, over a very small spatial scale, the resultant scattering will simply add to the diffuse background rather than to degradation of the small-angle image sharpness.

These considerations carry two implications as to technique development. First, deposits must be made to conform in geometry and thickness as closely as possible to the geometric form of the intended optical component, and second, deposits should be made on polished mandrels to minimize the lateral scale of any perturbation in the growth pattern. With these two controls, together with the maximum compositional control possible, we can expect a material certainly adequate for infrared systems use, and probably adequate for near i. r. and visible components.

c. Knoop Hardness

The Knoop hardness (using 50 gram or 200 gram load) was measured on samples taken from an area on the mandrel immediately adjacent to each of the lattice constant samples. The results of these hardness tests are given in Table III and the results of these tests as a function of composition are given in Fig. 9.

It is obvious from Fig. 9 that the hardness of ZnSe increases rapidly with small additions of substituted sulfur. Beyond a 20 mole percent substitution the rate of increase is not as rapid. A solid solution containing 10 percent sulfur has a Knoop hardness of ~200, while ZnSe has a value of approximately 90 - 95. For a 20 to 80 mole percent sulfur substitution the solid solution has a slightly higher hardness (~250) than ZnS. The spread in the data reflects the experimental accuracy of the hardness measurement, determination of composition from lattice constants, and grain size variations in these materials.

d. Flexural Strength

Strength measurements at room temperature were also carried out on representative samples from run ZSS-21 and -23 to further characterize the physical properties of these solid solutions. These tests were made on an Instron tensile test apparatus by standard 3-point and/or 4-point measurement techniques. The tests from run ZSS-23 are representative of 10 percent

TABLE III

KNOOP HARDNESS OF $Zn(S_{1-y}Se_y)$ SOLID SOLUTIONS

(50 gram load, kg/mm^2)

Run No.	Mixing Chamber	Bottom of Mandrel	Middle of Mandrel	Top of Mandrel
ZSS-4	- - -	- - -	195	- - -
ZSS-5	- - -	- - -	270	- - -
ZSS-6	- - -	- - -	265	- - -
ZSS-9	- - -	- - -	140	130
ZSS-11	157	145	100	115
ZSS-12	200	193	187	181
ZSS-13	249	243	236	230
ZSS-14	200	211	196	210
ZSS-15	200	258	247	240
ZSS-16	254	210	200	180
ZSS-17	203	228	200	200
ZSS-18	180	190	187	195
ZSS-19	- - -	200	200	185
ZSS-20	218	223	235	240
ZSS-21	219/225*	230/230*	230/230*	235/245*
ZS-67	- - -	- - -	286	- - -
ZS-47	- - -	- - -	278	- - -
ZSS-22	- - -	207	180	185
ZSS-23	- - -	187	190	188

*Substrate and deposition sides

26
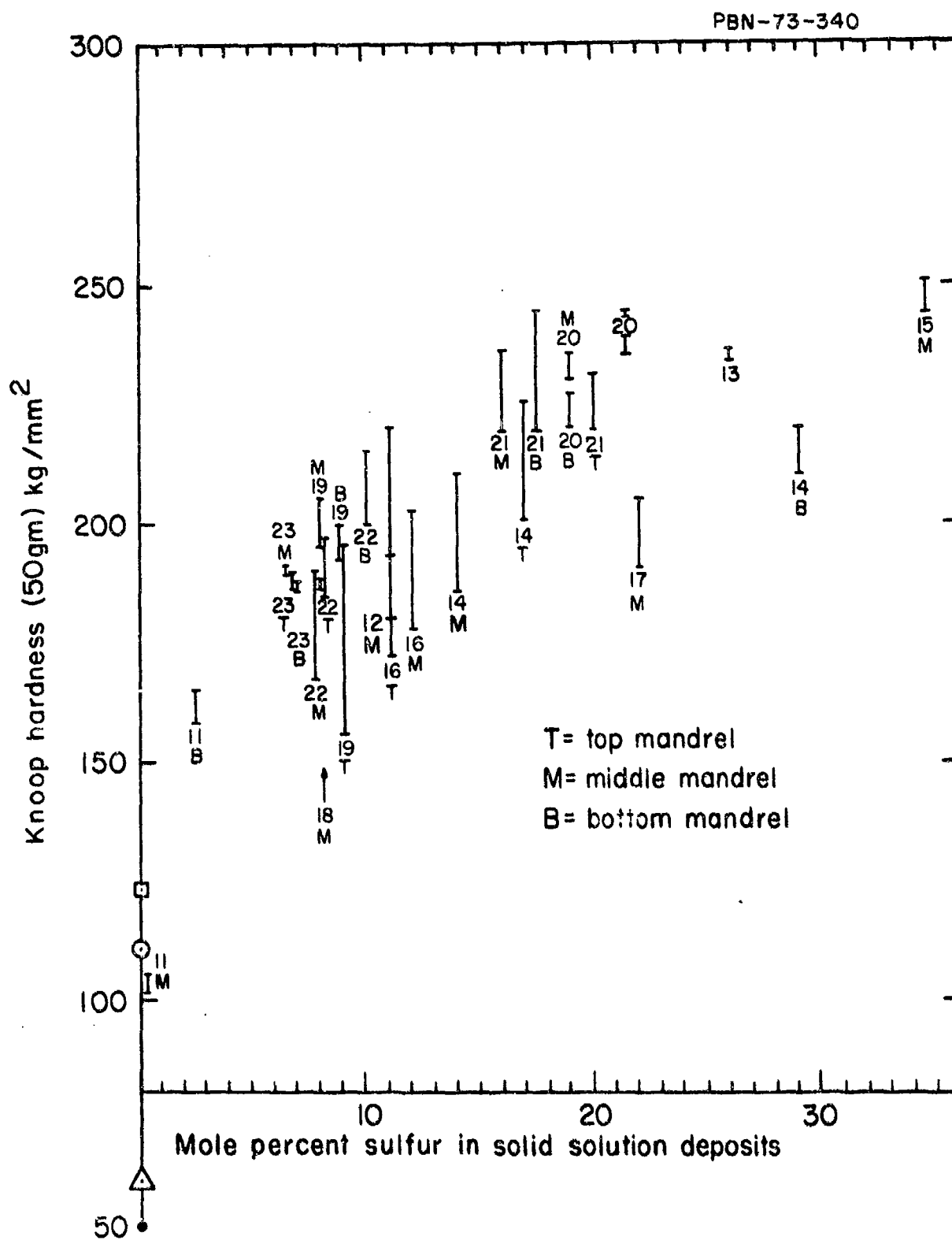
Fig. 9   Hardness as a Function of Composition for
Sulfo-Selenide Solid Solutions

27

substitution of sulfur for selenium ($ZnS_{0.1}Se_{0.9}$), while the test from ZSS-21 are representative of 20 percent sulfur substitution ($ZnS_{0.2}Se_{0.8}$).

Nine (9) polished beams of 0.25 × 0.05 in. cross-section from ZSS-23 were tested over a 1-1/2 in. span using 4-point loading. The results of these measurements are given in Table IV. The average strength of eight (8) of these beams is 7720 ± 780 psi. One beam yielded a value of 13,190 psi. We know that these strength results are extremely dependent on the surface quality of the beams being tested. Thus, in our opinion, the value of 7720 psi is low due to surface preparation, while the 13,190 value may be more representative of the true strength of the material.

Six (6) polished beams of 0.15 × 0.03 in. cross-section from ZSS-21 (20 percent sulfur substitution for selenium) were tested over a 2 in. span using 4-point loading and three of the same samples were tested using 3-point loading over a 1 in. span. The average strength of 4-point loaded samples was 9230 psi. As anticipated from hardness measurements, these strength values are higher than the specimens with a 10 percent sulfur substitution. Also these strengths represent values that are higher than pure ZnSe and they are equivalent to pure ZnS of the same grain size. Improvements in strength are anticipated as further refinement of the process conditions to achieve small grain size are realized.

Young's modulus was also determined for run ZSS-23 and was determined to be 9.16×10^6 psi.

e. Other Properties

The properties of CVD zinc-sulfo-selenide (10 percent sulfur substituted for selenium) are summarized in Table V along with the properties of the end members - zinc sulfide and zinc selenide.

The specific heat of a sample taken from ZSS-23 which represented a 7 percent sulfur substituted for selenium was submitted to Dynatech for

TABLE IV

ROOM TEMPERATURE FLEXURAL STRENGTH OF ZSS-23

(Four-Point Loading, 1-1/2 in. span)

	Sample No.	Flex. Strength (psi)
ZSS-23	1	13,187
	2	9,031
	3	7,471
	4	8,271
	5	8,376
	6	7,911
	7	6,462
	8	7,162
	9	7,049
	Avg.	7,717 ± 784 (spec. 2-9)

(Four-Point Loading, 2 in. span)

	Sample No.	Flex. Strength (psi)
ZSS-21	1	10,916
	2	8,464
	3	11,410
	4	7,895
	6	8,837
	7	7,854
	Avg.	9,229

(Three-Point Loading, 1 in. span)

	Sample No.	Flex. Strength (psi)
ZSS-21	5	8,710
	7	13,279
	8	12,335

TABLE V

CVD MATERIALS PROPERTIES

Property	Standard ZnSe	ZSS	ZnS
Density (gm/ cc)	5. 27	5. 15	4. 08
Refractive Index (8-13 μm)	2. 40	2. 38 (est.)	2. 20
Transmission (8-13 μm)	> 69%	(see transmission spectra)	
Transmission Limits	0. 5 - 22 μm	(see transmission spectra)	
Hardness (Knoop 50 gm, kg/ mm^2)	100	190	200
Absorption Coefficient at 10. 6 μm (cm^{-1})	0. 002-0. 005	0. 007	0. 22
Grain Size (microns)	250	100	(20 - 100)
Flexural Strength (psi, 4-point loading)	8500	----	11,100
Young's Modulus (psi, X10^6)	9. 75	9. 16	10. 8
Thermal Expansion (RT-500° C, X 10^{-6}/° C)	8. 53	8. 30	7. 85
Thermal Conductivity (RT)(cgs) 25° C	0. 043	0. 02	0. 040
Specific Heat (cal/ gm/° C)	0. 085	0. 083	0. 112
Electrical Resistivity (ohm-cm)	~10^{12}	~10^{12}	~10^{12}

measurement of specific heat. The sample was tested using Dynatech drop calorimeter. The heat capacity for this sample was 0.083 cal/gm/° C.

The thermal expansion of ZSS-23 ($ZnS_{0.07}Se_{0.93}$) was measured for the temperature range 25° to 500° C. Measurements were performed on a Leitz dilatometer with data points taken at 50° C intervals. The mean thermal expansion (RT-500° C) determined for this sample was 8.30×10^{-6}/° C.

The thermal conductivity for a sample from run ZSS-23, $3/4 \times 3/4 \times 1/4$ in. in size, was measured on a TPRC Model 100 Thermal Comparator. Samples of zinc sulfide and zinc selenide with known thermal conductivities were tested along with other standard samples for calibration of the instrument. The thermal conductivity determined for this sample was 0.02 cgs at 25° C.

The absorption coefficient of a sample taken from ZSS-23 was measured at 10.6 μm using standard laser calorimetry techniques. The absorption coefficient as determined by this measurement was 0.007 cm^{-1}.

The density of a sample from ZSS-23 as determined from lattice parameter measurements is 5.15 gm/cc. This value represents the density of a solid solution that has 10 mole percent sulfur substituted for selenium ($ZnS_{0.1}Se_{0.9}$).

3. ZINC-CADMIUM-SULFIDE SOLID SOLUTIONS

Another candidate material for multispectral window applications is zinc-cadmium-sulfide. As was the case for zinc-sulfo-selenide solid solutions, both end members of this system had been fabricated by the chemical vapor deposition process prior to the inception of the program. In contrast to the zinc-sulfo-selenide solid solutions, however, the crystal structure of zinc-cadmium-sulfide solid solutions is hexagonal and in order to deposit scatter-free material for use at visible wavelengths it is necessary that extremely fine-grain material be deposited. Another difference in this system

31

is that the multiphoron bands vary continuously as the composition of the material is shifted from zinc sulfide to cadmium sulfide.

Because of the different vapor pressures of zinc and cadmium it was necessary to make special provisions for the generation of the desired concentrations of each metal vapor species. Again, as in the zinc-sulfo-selenide system it was expected that the rates of reaction to form cadmium sulfide and zinc sulfide would be sufficiently different so that the final composition would have to be empirically determined by varying the ratios of the input metal species.

A separate apparatus was set up for these depositions which enabled us to control the temperature of the cadmium and zinc retorts independently. The zinc and cadmium vapors were generated in these retorts and passed into a heated mixing chamber prior to mixing them with H_2S gas to form the solid solution. Run ZCS-1 was a check-out run for purposes of determining furnace and retort temperature profiles. Six additional runs, ZCS-2 through -7, were exploratory runs where the process conditions were adjusted (see Table VI) periodically in an effort to establish favorable conditions to deposit a zinc-cadmium-sulfide solid solution. Analysis of the early runs indicated that the deposited material was all zinc sulfide or all cadmium sulfide. Only in run ZCS-7 was a solid solution deposited.

The composition of the zinc-cadmium-sulfide solid solutions were determined from X-ray lattice parameter analysis. Since it was surprising not to find any trace of cadmium in the initial runs, X-ray fluorescence analysis was also used to search for traces of cadmium in the deposit. In no case other than ZCS-5 and -7 was any cadmium fluorescence observed.

X-ray lattice parameters of a = 4.04 $\overset{\circ}{A}$, c = 6.57 $\overset{\circ}{A}$ indicated that the solid solution formed in ZCS-7 had an average composition of $(Zn_{0.3} Cd_{0.7})S$. Analysis of the X-ray data also indicated, however, that there was a variation in the composition from various areas of the deposit. ZCS-7 also showed a difference in properties both physical and optical when evaluated

TABLE VI

CVD $(Zn_{1-x}Cd_x)S$ RUNS

Run No.	Mandrel Temp (°C)	Furnace Press. (torr)	Zn Retort Temp (°C)	Cd Retort Temp (°C)	H_2S Flow (lpm)	Avg. Zn Pickup Rate (gm/hr)	Avg. Cd Pickup Rate (gm/hr)	Deposition Time (hrs)
ZCS-1	650	- - -	640	550	- - -	- - -	- - -	Furnace profile
ZCS-2	650	40	640/620	550/530	1.0	288	293	24
ZCS-3	650	80/60/40	640	550	1.0	163	83	20
ZCS-4	600/575/620	40	580	550	1.0	227	269	8/8/8-24
ZCS-5	580	40	580	550	1.0	68	378	12
ZCS-6	550	25	580	550	1.0	- - -	- - -	12/12-24
ZCS-7	540	30	550	525	1.0	100	250	24

on the substrate and deposition side. These differences in properties reflected compositional changes caused by adjustments that were made during the course of the run.

An analysis of the in-line transmission of this run allows some preliminary comments on the potential of this system as a candidate multispectral window material. Figure 10 compares the in-line transmission of 0.013 in. thick samples of CdS, ZnS, and the solid solution. The multiphonon region of these curves indicates that with the formation of a solid solution there is a progressive shift of the 15 to 17 μm absorption band and the other multiphonon bands of ZnS to longer wavelengths. It is also apparent that there is measurable scatter in these deposits, probably due to the presence of hexagonal phase.

Knoop hardness values were determined for all of the cadmium-zinc-sulfide deposition runs (Table VII). These data represent primarily the hardness of fine-grained ZnS with the exception of ZCS-7. The bottom side of this sample showed hardness value of 340 which is evidence of solid solution hardening. This high value is encouraging, but unless dramatic improvements are realized in the processing of this solid solution, it appears that it will not satisfy the optical requirements of a multispectral window for use at visible wavelengths.

4. IMPROVED ZnS

As discussed earlier in this report, zinc sulfide could function as a multispectral window provided that scatter at visible wavelengths could be reduced and the strength of the material could be increased so that thinner windows could be used. Under other Air Force Avionics Laboratory programs large plates of this material were fabricated and many of the initial problems encountered with its fabrication were resolved. Under this program, one of the remaining problems, optical uniformity (scatter) of the material in the thickness direction was investigated further.

34
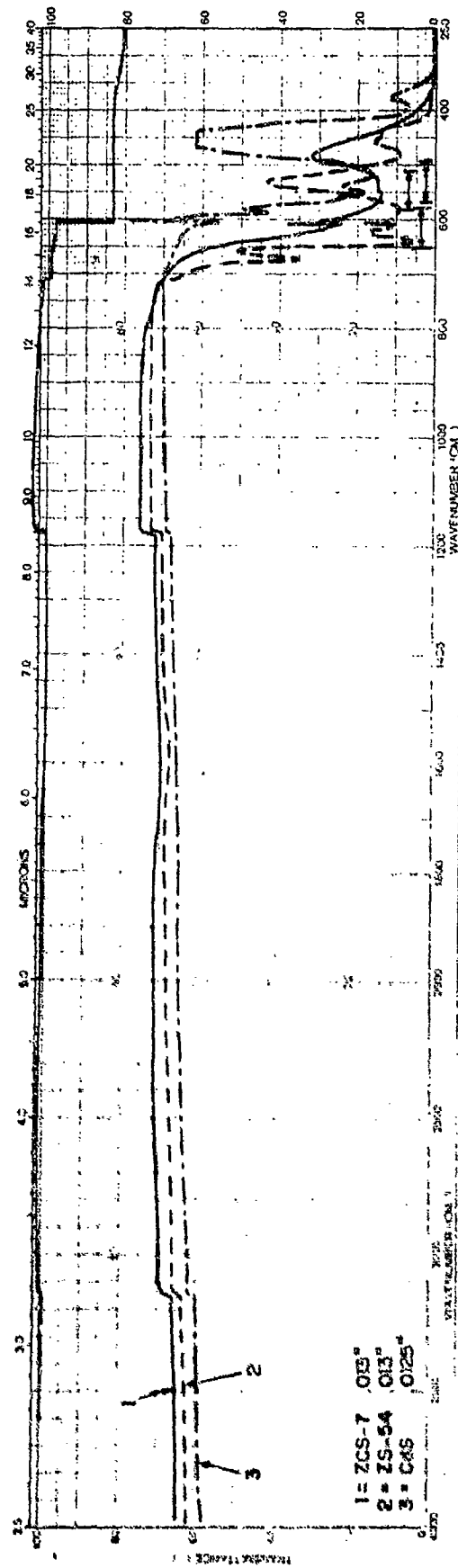
Fig. 10 Comparison of IR Transmission for ZnS, CdS and $(Zn_{0.3} Cd_{0.7})S$ Solid Solution ZCS-7

1 = ZCS-7 .013"
2 = ZS-54 .013"
3 = CdS   .0125"

TABLE VII

KNOOP HARDNESS

Sample No.	Position	Kn Hardness, kg/mm^2 (50-gm load)
ZCS-2	Middle of Mandrel	245
ZCS-3	Middle of Mandrel	230
ZCS-4	Middle of Mandrel	260
ZCS-6	Middle of Mandrel	270
ZCS-7	Middle of Mandrel	270, 340
ZSO-1	Exhaust Chamber	120
	Bottom of Mandrel	105
	Middle of Mandrel	110
	Top of Mandrel	100
ZSO-2	Exhaust Chamber	115
ZSG-1	Bottom of Mandrel	125
	Middle of Mandrel	120
	Top of Mandrel	118
ZSG-2	Mixing Chamber	125
	Top of Mandrel	160
ZnS/ZnO	5 μ ZnO on ZnS-93	340
ZnS/ZnO	10 μ ZnO on ZnS-93	590*
ZnSe/ZnO	5 μ ZnO on ZnSe-53	175
ZnSe/ZnO	10 μ ZnO on ZnSe-53	350

*200 gm load

When plates ~0.5 in. thickness are deposited, bands or layers of different imaging quality material are deposited. The nonuniformity is though to be caused by a nonuniform zinc usage rate as a function of time, sporadic gas phase reactions and/or the formation and dissociation of zinc hydride.

A nonuniform zinc usage rate is believed to be caused by the formation of a scum layer on the surface of the zinc melt. The scum layer is formed by an accumulation of impurities from the zinc (chiefly oxygen) and other furnace components that come in contact with the zinc. The problem is not necessarily resolved even with the use of 99.999 percent pure zinc since zinc oxide is the chief component of this surface slag. Various techniques were attempted during the course of the program to resolve this problem. Unfortunately none have been completely satisfactory. One retort design that was evaluated in run ZS-116 offers a potential solution to this problem. In this design a small amount of argon gas is bubbled through the zinc melt to keep the surface from forming a continuous layer. A larger flow of argon gas is simultaneously passed over the surface of the zinc melt to control the amount of zinc to be used per unit of time. This argon gas is passed into the zinc retort in such a manner that it is always at the same distance from the zinc surface. Furthermore, the usage rate can be directly measured as a function of time. If this retort will function for long periods of time as it performed for a portion of run ZS-116, it is felt that "bands" that are caused by nonuniform zinc usage can be eliminated and the good imaging quality material can be made in large plate sizes and at thicknesses of approximately 1/2 inch.

Run ZS-116 (Table I) was primarily concerned with depositing zinc sulfide at a lower deposition rate (0.002 to 0.003 in/hr) and a lower deposition temperature (600° C). Under these growth conditions it was expected that growth kinetics would be altered and that possibly a material with less scatter would result. This run yielded ~1/8 in. thick material with at least as good visible imaging quality material as any of the previous deposits with low H_2S/Zn molar input ratios. This is a promising approach to fabricating low scatter ZnS material that warrants further investigation.

In view of these results, other deposits made at deposition temperatures below 650° C were re-evaluated to determine their imaging characteristics, particularly in the visible. A review of these materials indicates that their imaging characteristics are better than 650° C deposited material. However, an additional problem arises when deposits are made at low temperatures. The problem is related to the design of the furnace. In all deposits the temperature of the zinc melt is maintained at or below the mandrel temperature. When the deposition temperature is decreased below 600° C it is difficult to achieve the desired molar ratio of zinc-to-hydrogen sulfide unless the retort is maintained at a temperature very close to, or higher than, the mandrel temperature. Thus it is possible to condense zinc as it enters into the deposition zone of the furnace. The net result is that finely dispersed particles of zinc are encapsulated in the final deposit. To circumvent this problem the furnaces would have to be modified. However, in view of the optical quality and strength (15, 000 psi) of the low temperature deposits, further work is warranted.

Runs ZS-117, -118 and -119 were exploratory runs that attempted to determine how the presence of zinc hydride influences the imaging characteristics of zinc sulfide. In the first run (ZS-117) hydrogen gas was added to the reaction. The addition of this gas should influence the dissociation of hydrogen sulfide and also enhance the formation of zinc hydride. The amount of scatter observed in this run was significantly greater than normal. Furthermore the 6.3 μm absorption band that we believe is due to zinc hydride was quite deep and exhibited structure. The other two runs (ZS-118 and -119) attempted to suppress the formation of zinc hydride. This was accomplished by adding oxygen to the reaction. In theory, the oxygen would oxidize any hydride that was formed. The results of this run were quite interesting. Colorless zinc sulfide with less scatter than normal was deposited, and the absorption band at 6.3 μm was practically annihilated. Further work in this area is obviously warranted.

Since some success had been achieved in depositing zinc-sulfo-selenide solid solutions with decreased scatter, two additional runs, ZSS-24 and -25,

were made to determine whether under these newly developed operating conditions zinc sulfide with only trace amounts of selenium would also yield good imaging quality material. The results of these two runs indicated that this was not the case, since the amount of scatter in the visible was similar to that experienced with standard deposits of zinc sulfide.

5. IMPURITY DOPED CVD ZnSe

    a. Oxygen Doped ZnSe

Based on annealing data (discussed in a later section), it appeared that zinc selenide could be hardened by the addition of zinc oxide. To determine whether this concept was valid two runs, ZSO-1 and -2, were made in which oxygen was added to H_2Se gas to codeposit ZnSe and ZnO (Table I).

The results of these runs were encouraging. Excellent imaging quality material was obtained and the in-line transmission (Fig. 11a) is similar to that observed for pure zinc selenide. The Knoop hardness (50 gm load) of the material was determined (Table VII) from various positions in the mandrel, and although somewhat variable, averaged approximately 115. Further work with this concept was not pursued since the cost of pure ZnSe at this time is prohibitive for multispectral window applications. Provided the hardness can be raised to an approximate value of 200 and the cost of ZnSe reduced, this concept is worthy of further work.

    b. Germanium Doped ZnSe

It also appeared feasible to harden ZnSe with germanium additions. The germanium would presumably be present as a second phase (Ge, or Ge_2Se_3). In two runs (Table I), ZGS-1 and -2, germane gas was added to the H_2Se gas to determine if a significant increase in hardening could be accomplished.
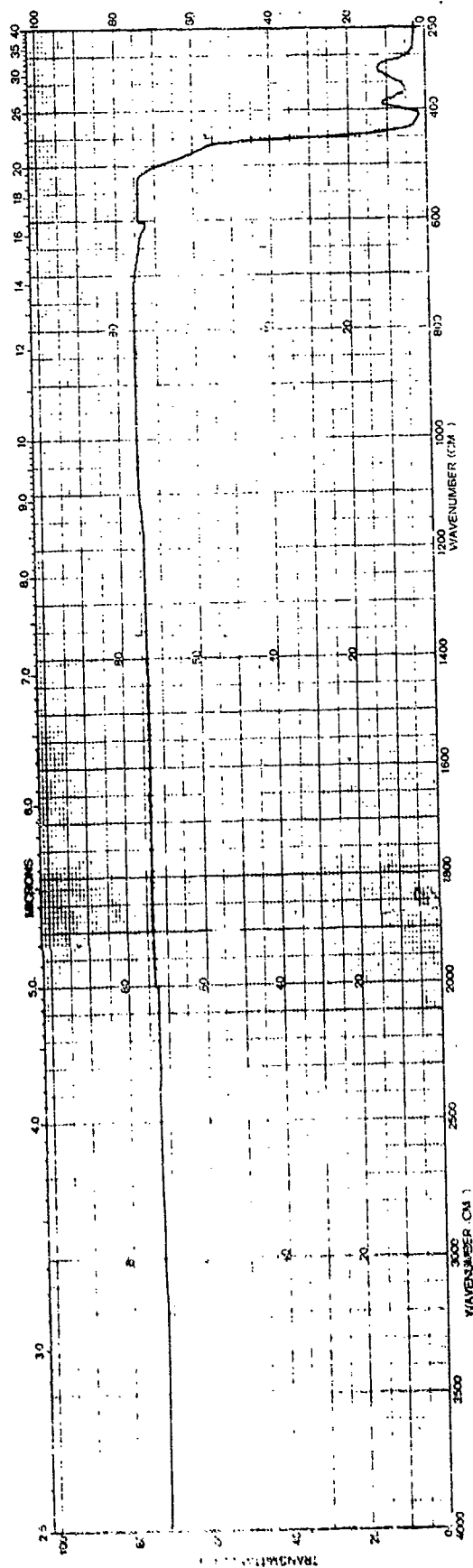
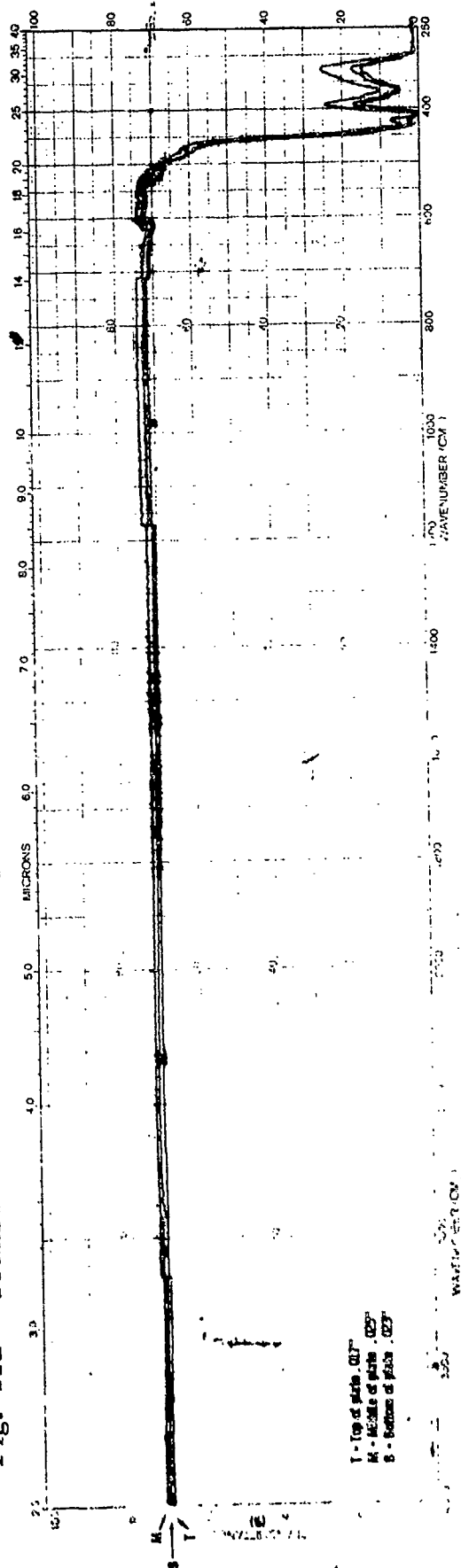Fig. 11a   Transmission of ZSO-1, Sample Thickness 0.027 in.

Fig. 11b   Transmission of Ge-Doped Zinc Selenide

40

The in-line transmission for ZGS-1 is shown in Fig. 11b and as noted, this material behaves optically similar to ZnSe. Hardness test data reported in Table VII indicate an apparent increase in hardness. This technique also warrants further investigation, but it was not pursued further in this program because of the projected high costs.

6. POST DEPOSITION ANNEALING STUDIES

a. Introduction

During the course of this investigation a large number of anneals were performed in an attempt to improve the homogeneity of solid solutions, to increase the hardness of zinc selenide, zinc sulfide, and solid solutions, and to improve the imaging quality of pure zinc sulfide. The annealing conditions used are summarized in Table VIII.

b. Solid Solution Annealing

Following the deposition of the initial zinc-sulfo-selenide solid solutions with their poor imaging and homogeneity characteristics, it was theorized that improvements might be realized through heat treatment. Originally it was felt that the imaging characteristics of the homogeneous cubic solid solutions should be at least as good as the end members. From X-ray data that show line broadening it was known that the solid solutions were not completely homogeneous. Two solid solution compositions [$Zn(Se_{0.1}S_{0.9})$ and $Zn(Se_{0.9}S_{0.1})$] were annealed under a variety of conditions. After the anneal treatment the lattice parameter and X-ray line broadening was remeasured. The results of these anneals was to effectively further degrade their homogeneity and imaging quality. It is theorized that the cause of the degradation was due to the preferential evaporation of selenium from the samples. Adjustments to the partial pressure of selenium over these compositions necessary to stop preferential evaporation was not carried out since another set of anneals indicated that when this was done a surface layer formed which exhibited signficant scatter.

41

TABLE VIII

SUMMARY OF ANNEALING CONDITIONS FOR ZnSe, ZnS AND SOLID SOLUTIONS

Anneal Run	Temp (°C)	Time (hrs)	Atmosphere							
			Air	Vacuum	Zn	S	Se	Te	Se + S	H_2S
No. 10	800	24			ZSS-6(3) ZSS-6(2) ZSS-7	ZnSe-40 ZnSe-40	ZnSe-40 ZS-89 ZnSe-40			ZnS-90 ZnS-90*
No. 11	600	24	ZnS-90	ZnSe-40		ZnSe-40	ZnSe-40	ZnSe-40	ZnSe-52 (Se:200 mm, S: 560 mm) ZnSe-52 (Se:400 mm, S: 360 mm) ZnSe-52 (Se:600 mm, S: 160 mm)	
No. 12	800	24		ZnS-91(3)			ZnS-91	ZS-89 ZnSe-40	ZnS-91 (Se: 400, S:360) ZnS-91 (Se: 600, S:160)	
No. 13	850	24			ZnSe-40 ZnS-91					
No. 14	400	24 48 72	ZnSe-52(2) ZnSe-52			ZnS-91				
No. 15	900			ZnS-91						
No. 16	650			ZnS-91						ZnS-90
No. 17	600	16								ZnS-112 ZnS-116
No. 16	600	30								ZnS-112 ZnS-116

*600° C

42

c. Bleaching Zinc Sulfide

It was known from previous studies that the absorption at 0.4 to 0.5 μm that gives rise to the yellow coloration in zinc sulfide, as well as the 6.3 μm infrared absorption band, could be annealed out by post deposition treatments in sulfur-containing atmospheres. Some effort was expended during the course of this study to establish an annealing condition which would enable us to fabricate colorless zinc sulfide at thicknesses of 1/4 to 1/2 inch. Various annealing treatments in a dynamic vacuum, low oxygen partial pressures, sulfur, and low hydrogen sulfide partial pressure atmosphere, led to the disappearance of the 6.3 μm absorption band as well as the coloration of the material. A summary of the various anneals performed are presented in Table VIII. The most promising annealing condition is a low hydrogen sulfide partial pressure at a temperature near the actual deposition temperature. For example, an 1/8 in. thick sample from run ZS-116 was annealed so that it was colorless throughout in 30 hrs at a temperature of 600° C (see anneal No. 18, Table VIII). The resultant materials, upon close examination, however, appear to scatter slightly more than as-deposited material.

d. Hardened Zinc Selenide

A number of post deposition treatments were also tried in an effort to harden the surface of zinc selenide by a diffusion technique. For these experiments, polished samples of the material were placed in sealed quartz ampoules (when appropriate) and annealed in atmospheres of free sulfur, tellurium, oxygen, zinc, dynamic vacuum, air, and various mixtures of selenium and sulfur (see Table VIII). In-line transmission curves for each of these samples were measured before and after the anneals. In some of the samples significant hardening was observed after annealing (Table IX). In some cases the annealing caused an etching (and thus scattering) of the surface, and in other cases a high scatter layer of a different composition was formed on the surface. Repolishing of the samples to remove the surface layers removed the hardened layer and returned the surface to the hardness of the substrate material. Typical transmission curves for zinc selenide

43

TABLE IX

SUMMARY OF POST-DEPOSITION ANNEALS

Sample Description	Anneal Atmosphere	Anneal Temp. (° C) (for 24 hrs)	Knoop Hardness (50 gm)
ZnSe-16	No anneal (660° C Mat'l)	---	122
ZnSe-41	No anneal (750° C Mat'l)	---	103
ZnSe	Irtran-4	---	116
ZnS-39	No anneal (750° C Mat'l)	---	213
ZnS-45	No anneal (650° C Mat'l)	---	240
ZnS	Irtran-2	---	240
ZnS-89	No anneal (clear CVD ZnS)	---	264
ZnS-91	No anneal (yellow CVD ZnS)	---	227
ZSS-7	No anneal (CVD $Zn(S_{.1}Se_{.9})$)	---	221
ZnS-89	Se atm, #10	800	410
ZSS-6	$Zn(Se_{.1}S_{.9})$ Zn atm, #10	800	830*
ZSS-6	$Zn(Se_{.1}S_{.9})$ Zn atm, #10	800	272
ZSS-7	$Zn(Se_{.9}S_{.1})$ Zn atm, #10	800	220
ZnS-89	Te atm, #12	800	275
ZnS-91	Zn atm, #13	850	220
ZnSe-40	750° C ZnSe, S atm, #10	800	263
ZnSe-40	750° C ZnSe, Se atm, #10	800	116
ZnSe-40	750° C ZnSe, Vac., #10	800	105
ZnSe-40	750° C ZnSe, S atm, #11	600	262
ZnSe-40	750° C ZnSe, Se atm, #11	600	105
ZnSe-40	750° C ZnSe, Te atm, #12	800	133
ZnSe-40	750° C ZnSe, Zn atm, #13	850	108
ZnSe	No anneal	No anneal	110
ZnSe	S (760 mm)	400	225
ZnSe	Te (76 mm)	800	133
ZnSe	Zn (400 mm)	850	108
ZnSe	S+Se (P_T = 760 mm)	600	193
ZnS	No anneal	No anneal	224
ZnS	S (400 mm)	400 (72 hrs)	249
ZnS	S+Se (P_T = 760 mm)	800	249

*Slight oxygen leak

Table IX (Cont'd)

Sample Description	Anneal Atmosphere	Anneal Temp. (° C) (for 24 hrs)	Knoop Hardness (50 gm)
ZnS	Se (760 mm)	800	237
ZnS	Dynamic vacuum	800	253
ZnS	Zn (400 mm)	850	220
ZnSe	Dynamic vacuum (25 μ)	600	105
ZnSe	Se (760 mm)	600	105
ZnSe	Se (760 mm)	800	105
ZnSe	Air (760 mm)	400	131
ZnS	Dynamic vacuum (25 μ)	650	270
ZnS	Air (760 mm)	600	262
ZnS	H_2S (760 mm)	650	235
ZnS	H_2S (760 mm)	800	190
ZnS	H_2S (760 mm)	600	275

before and after an annealing treatment are shown in Fig. 12a. Other anneal-
ing treatments gave similar results.

e. Hardened Zinc Sulfide

As in the case of zinc selenide, zinc sulfide samples were annealed
in various atmospheres in order to increase hardness. The results of these
annealing treatments were similar to those for zinc selenide. Table IX in-
cludes the hardness data for these annealed samples. The most significant
increase in hardness observed was obtained when the material was annealed
in oxygen (Table IX). Figure 12b shows a typical transmission curve of
as-deposited zinc sulfide before and after an anneal in a dynamic vacuum.

f. Oxide Surface Coatings

Specimens annealed in air, and those that have had a layer of zinc
oxide sputtered on their surface, have yielded data that may be pertinent to
the usefulness of these materials in FLIR applications. Figure 13a shows
the transmittance of a ZnSe specimen heated in air at 400° C. It is estimated
that an oxide coating of 2 μm has been formed on the surface. At the shorter
wavelengths a higher transmittance is observed because the index of refrac-
tion of the coating is lower than that of the zinc selenide. At the longer
wavelengths the coated material has a transmittance to 11.5 μm equivalent
to that of ZnSe. The Knoop hardness (50 gm load) of this material was de-
termined to be 131 (Table IX). The Knoop hardness of uncoated ZnSe is 95
to 110.

A typical transmittance curve of ZnS with a 5 μm sputtered layer of
ZnO is shown in Fig. 13b. As noted from this curve, a typical interference
curve has been obtained and in order to be useful, either a double layer or
a layer of a different thickness would be needed for maximum transmission
between 8 and 12 μm. The Knoop hardness (50 gm load) of this sample was
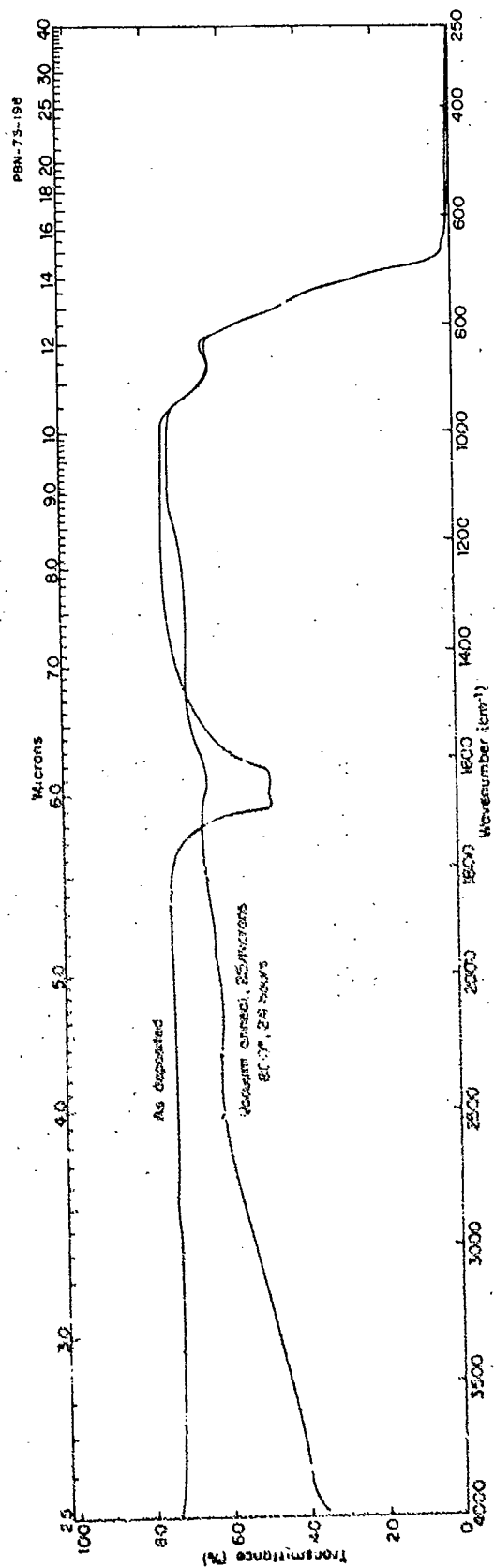determined to be 340 (Table IX).

46

Fig. 12a   Transmittance of ZnS-91 Before and After Post Deposition Treatment.
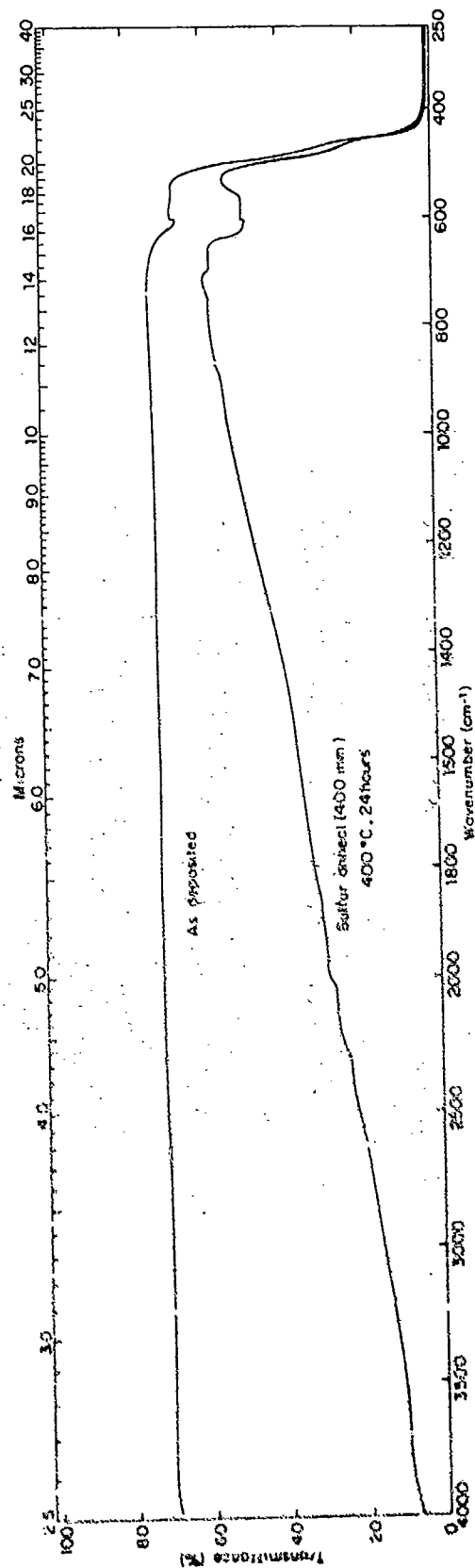   Sample thickness 0.202 in.

Fig. 12b   Transmittance of ZnSe-40 Before and After Post Deposition Treatment.
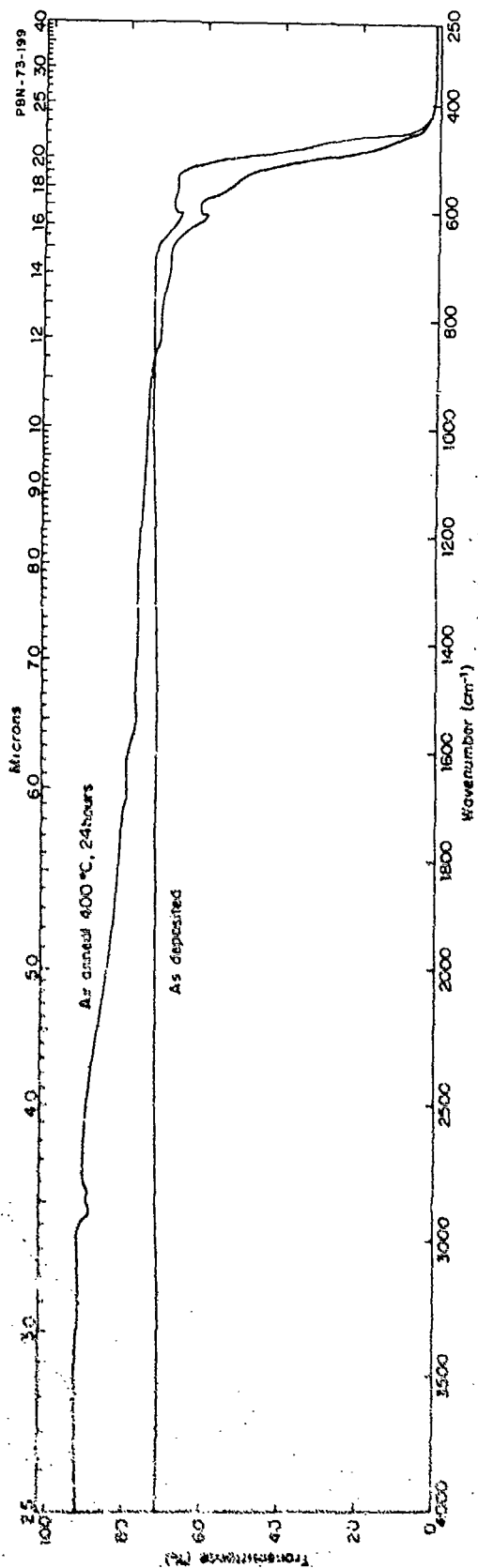   Sample thickness 0.088 in.

47

Fig. 13a   Transmittance of ZnSe-52 Before and After Post Deposition Treatment.
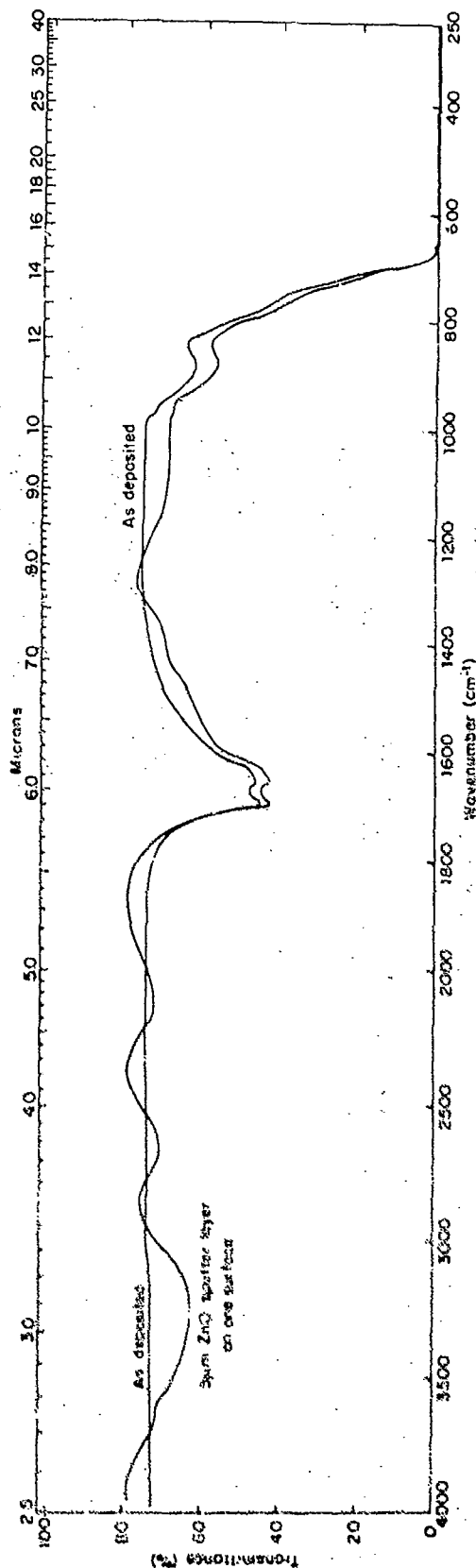Sample thickness 0.107 in.

Fig. 13b   Transmittance of ZnS-93 Before and After Post Deposition Treatment.
Sample Thickness 0.200 in.

The usefulness of either type of coating on ZnS, ZnSe and solid solutions obviously needs further evaluation. Figure 14 indicates the increase in hardness as a function of film thickness that has been observed in ZnS and ZnSe. It remains to be seen how thick a coating is needed to improve the rain erosion characteristics of the material. Furthermore, as the coating thickness is increased there undoubtedly will be absorptions at certain wavelengths. This optical degradation will have to be traded-off against environmental survival.

7. DELIVERABLE HARDWARE

As described in an earlier section, run ZSS-23 was primarily made for the purpose of fabricating plates for delivery to the Air Force Avionics Laboratory. In this run deposition was carried out for 47 hours in order to obtain a sufficient deposit to fabricate a plate approximately 1/4 in. thick. This run was successful and yielded two plates $2 \times 4 \times 0.228$ in., plus sufficient material to allow the fabrication of samples for property measurements described previously. Table V lists these properties along with the properties of zinc sulfide and zinc selenide for comparison. The transmission of a polished plate $2 \times 4 \times 0.228$ in. was measured from 0.3 μm to 40 μm. Transmission measurements were made at three different locations on the plate and all were coincident indicating good homogeneity over this area. Figure 8 shows the typical transmission curve that was determined. Figure 15 shows one of these $2 \times 4 \times 1/4$ in. plates polished to a 1/4 wave surface. In addition to these two plates, a 2×4 in. plate of improved ZnS was also submitted for further evaluation by the Air Force Avionics Laboratory. This material was deposited in run ZS-116.
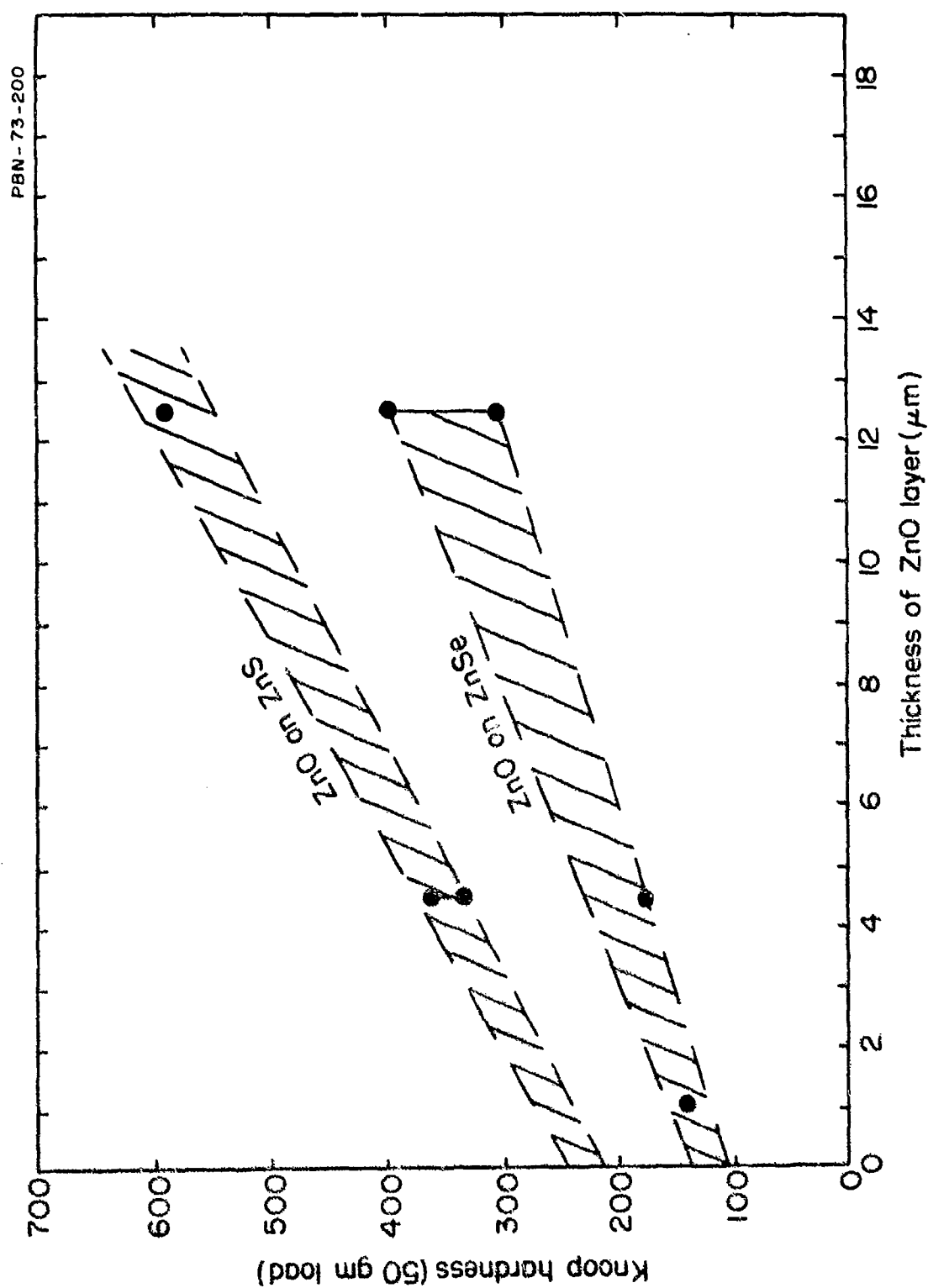
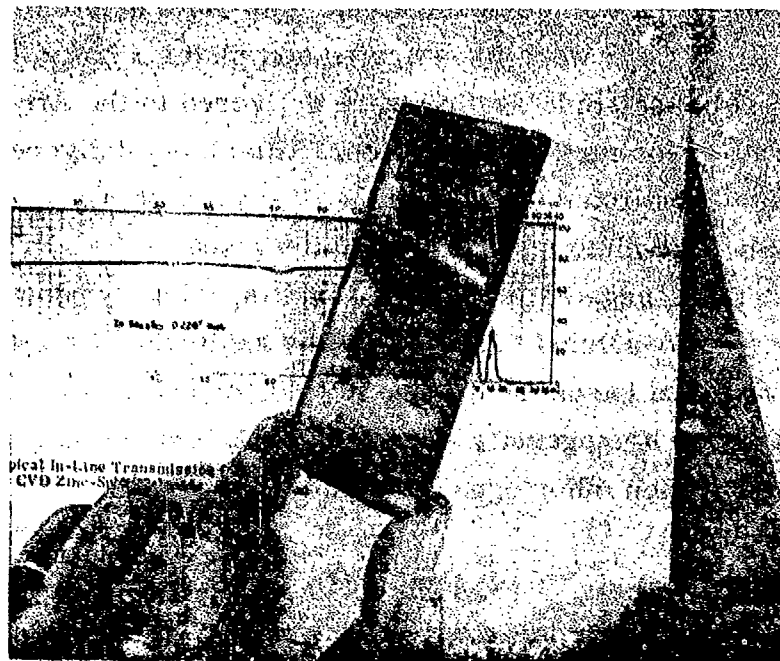Fig. 14   Surface Hardness of ZnS and ZnSe as a Function of ZnO Surface Thickness

50

Fig. 15   2 in. × 4 in. × 0.228 in. $ZnS_{0.07}Se_{0.93}$ Plate

SECTION IV
CONCLUSIONS

The feasibility of using the chemical vapor deposition process to fabricate solid solutions was demonstrated. Two solid solution systems, $ZnSe_{1-x}S_x$ and $Zn_{1-y}Cd_yS$ were investigated and plates 2 X 4 X 0. 25 in. in size of the zinc sulfo-selenide system were delivered to the Air Force Avionics Laboratory for further evaluation. The plates delivered had seven (7) percent sulfur substituted for selenium. Even though a solid solution was formed in the zinc-cadmium sulfide system the amount of scatter observed at visible wavelengths negated its use as a multispectral window at this time. In contrast, zinc sulfo-selenide solid solutions exhibit less scatter, have an equivalent strength and hardness to zinc sulfide, and transmit to ~13 μm. Some improvement in homogeneity is needed to eliminate a potentially bothersome index of refraction inhomogeneity problem.

The addition of either oxygen or germanium to zinc selenide apparently increases its hardness without degrading its excellent optical properties. The concept of improving the structural properties of CVD zinc selenide by this method were not fully explored since the cost of this material for multispectral windows was considered to be prohibitive at this time. Nevertheless, the concept should be more fully explored.

Exploratory runs made to decrease the amount of scatter in zinc sulfide also proved to be successful. A decreased deposition rate, deposition temperature, a uniform zinc usage rate, and a lack of gas phase reaction appear to be the most important variables that control the amount of scatter. The addition of oxygen to the reaction produced a colorless material with reduced scatter. Equivalent type material can be produced by post deposition annealing in a hydrogen sulfide atmosphere.

Finally, it was found that the surface hardness of all the materials deposited could be significantly increased by oxidizng them at ~400° C. It remains to be determined how thick a coating is needed to improve their rain erosion characteristics.

SECTION V
RECOMMENDATIONS

It has been demonstrated that the chemical vapor deposition process can be used to fabricate solid solutions of II-VI compounds. Plates of 2 X 4 X 0.25 in. size of $ZnSe_{0.93}S_{0.07}$ composition were fabricated and delivered to the Air Force Avionics Laboratory. The potential of this system should be further exploited by improving its optical quality (scatter and homogeneity) and determining an optimum composition. These improvements can be accomplished by the following experiments.

1) Better control of the zinc usage rate.

2) Better mixing of the reactants by modification of the furnace.

3) Elimination or minimization of gas phase reactions.

4) Elimination or minimization of growth nodules through use of optically polished metal mandrels.

5) Increased hardness and strength through substitution of higher percentages of sulfur for selenium.

6) Cost reduction of material by increasing the amount of sulfur and by better utilization of the reactants.

Precipitation hardening of zinc selenide should also be explored further with the use of oxygen, germanium, or arsenic.

Finally, techniques to decrease the amount of scatter in zinc sulfide should be explored again. Under the appropriate operating conditions (low deposition temperature, low deposition rate, minimized gas phase reactions, oxygen gas addition, a significant decrease in the amount of scatter was observed.

DISTRIBUTION LIST

No. of Copies	
2	DDC Cameron Station Cameron Station Alexandria, VA 22314
3	AFAL/TEL-1 (C. T. Ennis) Wright-Patterson AFB, OH 45433
1	Defense Ceramic Information Center Battelle Memorial Inst. Room 11-9021 505 King Avenue Columbus, OH 45201
1	AFAL/TSR Wright-Patterson AFB, OH 45433
1	2700th ABW/SSL Wright-Patterson AFB, OH 45433
1	Air University Library Maxwell AFB, AL 36112
1	Hq USAF (SAMID) Washington, DC 20330
1	AFAL/RSP-4 (ATTN: Mr. M. Carr) Wright-Patterson AFB, OH 45433
1	Perkin-Elmer Co. ATTN: E. Strouse 77 Danbury Road Wilton, CT 06897
1	General Electric Company ATTN: E. L. Bartels P. O. Box 2143 Kettering Branch Dayton, OH 45429
1	Martin Marietta Corp. ATTN: Mr. D. R. Maley P. O. Box 5837 Orlando, Florida 32805

No. of Copies

1   Hughes Aircraft Company
Aerospace Group
Missile System Division
ATTN: Mr. V. F. Olson
Canoga Park, California

1   Texas Instruments, Inc.
Equipment Group
Electro-Optics Division
ATTN: Mr. Bob Crossland
P. O. Box 6015
Dallas, Texas 75222

4   ASD/RWRS
ATTN: Lt. Col. James R. Wolverton
SCANA Program Office
Directorate of Recon/Strike Projects
Wright-Patterson AFB, OH 45433

DOCUMENT CONTROL DATA - R & D

(Security classification of title, body of abstract and indexing annotation must be entered when the overall report is classified)

1. ORIGINATING ACTIVITY (Corporate author)	2a. REPORT SECURITY CLASSIFICATION
Raytheon Company Research Division Waltham, Massachusetts	UNCLASSIFIED
	2b. GROUP N/A

3. REPORT TITLE

Chemical Vapor Deposition of Multispectral Windows

4. DESCRIPTIVE NOTES (Type of report and inclusive dates)
Final Technical Report, May 1972 to May 1973

5. AUTHOR(S) (First name, middle initial, last name)

Bernard A. diBenedetto, James Pappis, Anthony J. Capriulo

6. REPORT DATE	7a. TOTAL NO. OF PAGES	7b. NO. OF REFS
July 1973	53	0

8a. CONTRACT OR GRANT NO. F33615-72-C-1501	9a. ORIGINATOR'S REPORT NUMBER(S)
b. PROJECT NO. 6102	S-1580
c.	9b. OTHER REPORT NO(S) (Any other numbers that may be assigned this report) AFAL-TR-73-252
d.	

10. DISTRIBUTION STATEMENT
Distribution limited to U. S. Government agencies only; report contains test and evaluation information, July 1973. Other requests for this document must be referred to AFAL/TEL, Wright-Patterson AFB, Ohio.

11. SUPPLEMENTARY NOTES	12. SPONSORING MILITARY ACTIVITY
N/A	Air Force Avionics Laboratory Air Force Systems Command Wright-Patterson AFB, Ohio

13. ABSTRACT

   The significance of this research and development program to the Air Force is the demonstrated feasibility of fabricating zinc sulfo-selenide solid solutions for use as multispectral windows. Plates of $2 \times 4 \times 0.25$ in. in size with good transmission properties over the entire spectrum were made and delivered. Furthermore, the strength and hardness of the solid solution is equivalent to zinc sulfide. Some improvement in homogeneity is needed, however, before an engineering material is available for systems use.

   It was also shown that the hardness of pure zinc selenide could be increased by the use of oxygen or germanium. Finally, the amount of scatter in zinc sulfide was found to be dependent on deposition temperature, deposition rate, zinc usage rate, and the amount of gas phase reaction occurring during deposition.

DD FORM 1473, 1 NOV 65

14. KEY WORDS	LINK A		LINK B		LINK C	
	ROLE	WT	ROLE	WT	ROLE	WT
Reconnaissance						
Zinc-sulfo selenides						
Optical windows						
FLIR						
Multispectral						